

# **3D Rendering of the Regional Stratigraphy of Paleogene–Quaternary Sediments in West-Central Alberta**

**AER/AGS Report 93**

# **3D Rendering of the Regional Stratigraphy of Paleogene–Quaternary Sediments in West- Central Alberta**

L.A. Atkinson and G.M.D. Hartman

Alberta Energy Regulator  
Alberta Geological Survey

April 2017

©Her Majesty the Queen in Right of Alberta, 2017  
ISBN 978-1-4601-0170-4

The Alberta Energy Regulator/Alberta Geological Survey (AER/AGS), its employees and contractors make no warranty, guarantee or representation, express or implied, or assume any legal liability regarding the correctness, accuracy, completeness or reliability of this publication. Any references to proprietary software and/or any use of proprietary data formats do not constitute endorsement by AER/AGS of any manufacturer's product.

If you use information from this publication in other publications or presentations, please acknowledge the AER/AGS. We recommend the following reference format:

Atkinson, L.A. and Hartman, G.M.D. (2017): 3D rendering of the regional stratigraphy of Paleogene–Quaternary sediments in west-central Alberta; Alberta Energy Regulator, AER/AGS Report 93, 44 p.

**Published April 2017 by:**

Alberta Energy Regulator  
Alberta Geological Survey  
4th Floor, Twin Atria Building  
4999 – 98th Avenue  
Edmonton, AB T6B 2X3  
Canada

Tel: 780.422.1927  
Fax: 780.422.1918  
E-mail: [AGS-Info@aer.ca](mailto:AGS-Info@aer.ca)  
Website: [www.ags.aer.ca](http://www.ags.aer.ca)

## Contents

|   |     |
|---|-----|
| Acknowledgements.....   | vi  |
| Abstract.....   | vii |
| 1 Introduction.....   | 1   |
| 2 Study Area Characteristics.....   | 1   |
| 2.1 Physiography.....   | 1   |
| 3 Geological Background.....  | 4   |
| 3.1 Upper Cretaceous–Paleogene Bedrock Geology.....                                   | 4   |
| 3.2 Paleogene–Quaternary Geology.....   | 4   |
| 3.2.1 Preglacial Geological History.....  | 4   |
| 3.2.2 Laurentide-Cordilleran Glacial Geological History.....                          | 6   |
| 4 Methodology.....  | 7   |
| 4.1 Lithological Database.....  | 9   |
| 4.1.1 Calibration of Variable Quality Data with Field Observations.....               | 9   |
| 4.2 Cross-Section Analysis and Model Construction.....                                | 9   |
| 4.2.1 Bedrock Topography Modelling.....   | 9   |
| 4.2.2 Paleogene–Quaternary Stratigraphic Unit Modelling.....                          | 12  |
| 5 Bedrock Topography and Sediment Thickness.....                                      | 12  |
| 6 Paleogene–Quaternary Stratigraphy.....  | 14  |
| 6.1 SU1/SU2: Gravel Overlying Bedrock on Benchlands and Plains.....                   | 15  |
| 6.2 SU3: Buried-Valley Gravel Deposits.....   | 20  |
| 6.3 SU4a: Coarse-Grained Glaciogenic Diamict.....                                     | 20  |
| 6.4 SU4b: Fine-Grained Glaciolacustrine Silt, Clay, and Diamict.....                  | 28  |
| 6.5 SU5: Fluvial and Glaciofluvial Sand and Gravel and Eolian Sand.....               | 32  |
| 7 Model Limitations and Uncertainty.....  | 36  |
| 8 Development of a Hydrostratigraphic Model of the Paleogene–Quaternary Deposits..... | 36  |
| 9 Conclusions.....  | 39  |
| 10 References.....  | 40  |

## Tables

|   |    |
|---|----|
| Table 1. Sediment characteristics and model summary statistics of Paleogene–Quaternary stratigraphic units..... | 15 |
| Table 2. Selected grain size results from SU1 and SU4a.....   | 17 |
| Table 3. RMSE values for gridded surfaces used to construct 3D model.....                                       | 38 |

## Figures

|  |   |
|--|---|
| Figure 1. A hill-shaded digital elevation model (DEM) of the land surface in the study area showing major geographic features referred to in the text.....   | 2 |
| Figure 2. Physiographic districts and major drainage basins. Cross-section A-A' displays the surface topography of benchlands and plains.....  | 3 |
| Figure 3. Bedrock geology map of WCAB and adjacent areas. Cross-section A-A' illustrates the wedge-shaped geometry of bedrock units and their relationship with the physiographic regions in the study area..... | 5 |
| Figure 4. Generalized Cordilleran Ice Sheet (CIS) and Laurentide Ice Sheet (LIS) glacial flow lineations and suture zone.....  | 6 |
| Figure 5. Surficial geology map of WCAB and adjacent areas.....  | 8 |

|            |   |    |
|------------|---|----|
| Figure 6.  | Hill-shaded bare-earth LiDAR DEM showing locations of (a) borehole data compiled in the lithological database and (b) field data collected by the AGS. ....   | 10 |
| Figure 7.  | A digital elevation model (DEM) of the bedrock topography of the study area and location of input data. ....  | 11 |
| Figure 8.  | (a) A hill-shaded DEM of the WCAB bedrock topography showing paleovalley thalwegs. (b) Sediment thickness map of the Paleogene–Quaternary succession. ....  | 13 |
| Figure 9.  | 3D view of modelled Paleogene–Quaternary stratigraphic units overlying bedrock. Characteristics of units are described in Table 1. ....   | 14 |
| Figure 10. | (a) Hill-shaded bare-earth LiDAR DEM showing SU1/SU2 data locations and modelled extent. (b) Detailed view of the SU1 isopach across benchland steps and the location of AGS boreholes. Lithological descriptions and gamma-ray log from AGS borehole WCAB-15-03 in which SU1 was identified. (c) Outcrop showing the contact of SU1 and SU4a, AGS field site GH15-16. .... | 16 |
| Figure 11. | Hill-shaded bare-earth LiDAR DEM showing the elevation of SU1. ....   | 18 |
| Figure 12. | Hill-shaded bare-earth LiDAR DEM showing the thickness of SU1. ....   | 19 |
| Figure 13. | Modelled extent of SU3 and location of paleovalley thalwegs overlain on a hill-shaded DEM of the bedrock topography. Cross-section B-B' shows SU3 within the High Prairie paleovalley. ....   | 21 |
| Figure 14. | Hill-shaded bare-earth LiDAR DEM showing the elevation of SU3. ....   | 22 |
| Figure 15. | Hill-shaded bare-earth LiDAR DEM showing the thickness of SU3. ....   | 23 |
| Figure 16. | Portions of floodplain and terraces of the preglacial Grizzly Valley (SU3) remain recognizable along this part of the Little Smoky Valley in western WCAB (inset A) even though they are superposed by an esker and meltwater channel (SU5) and scattered glacial deposits (SU4a), and are incised by the modern river (SU5). ....  | 24 |
| Figure 17. | (a) Outcrop description and AGS stratigraphic interpretation. (b) 3D view of SU4a overlying bedrock. (c) Photo of AGS field site showing exposure of SU4a. ....   | 25 |
| Figure 18. | Hill-shaded bare-earth LiDAR DEM showing the elevation of SU4a. ....  | 26 |
| Figure 19. | Hill-shaded bare-earth LiDAR DEM showing the thickness of SU4a. ....  | 27 |
| Figure 20. | (a) Stratigraphic interpretation of ARC coal-survey borehole litholog and geophysical log. (b) Modelled extent of SU4b overlain on the hill-shaded bare-earth LiDAR DEM with the outlines of glacial lakes. (c) Photo of AGS field site with interpreted stratigraphic unit SU4b. ....  | 29 |
| Figure 21. | Hill-shaded bare-earth LiDAR DEM showing the elevation of SU4b. ....  | 30 |
| Figure 22. | Hill-shaded bare-earth LiDAR DEM showing the thickness of SU4b. ....  | 31 |
| Figure 23. | (a) Surficial map showing the distribution of eolian, fluvial, and glaciofluvial sediments, classed as SU5, and the location of cross-section C-C'. (b) Cross-section C-C' of the model shows SU5 infill of a valley incised into bedrock along the present-day Berland River. (c) Photos of AGS field sites showing exposure of sediments classed as SU5. ....             | 33 |
| Figure 24. | Hill-shaded bare-earth LiDAR DEM showing the elevation of SU5. ....   | 34 |
| Figure 25. | Hill-shaded bare-earth LiDAR DEM showing the thickness of SU5. ....   | 35 |
| Figure 26. | Sources of error contributing to model uncertainty. ....  | 37 |
| Figure 27. | Density of input data. ....   | 38 |

## Acknowledgements

The authors wish to acknowledge the following individuals for their contributions to this report:

- L. Andriashek (AGS) aided in AGS drilling and helicopter investigations. His helpful discussions during the development and progression of the study were greatly appreciated, as well as his constructive comments on earlier versions of this report.
- T. Playter and B. Smerdon (AGS) conducted fieldwork during the AGS drilling investigation.
- A. Hughes and D. Smyth (AGS summer students) helped with fieldwork during the summer of 2015.
- S. Pawley, D. Utting, and N. Atkinson (AGS) collected surficial field data.
- U. Wityk (AER contract employee) digitized legacy AGS data.
- S. Stewart (AGS) compiled the Alberta Water Well Information Database into usable format for this study.
- Scientific review provided by L. Andriashek, N. Atkinson, B. Smerdon and M. Grobe (AGS).
- Editorial review by A. Dalton (AER) and M. Grobe (AGS).

## Abstract

A 3D geological model of Paleogene–Quaternary sediment units has been rendered for west-central Alberta as part of a combined geological and hydrogeological study in the region. The study integrates previously conceptualized stratigraphic units in the Paleogene–Quaternary succession with new interpretations into a 3D model. Shallow subsurface data that include multisource borehole and field data containing lithological descriptions, geospatial datasets in GIS format, and published gridded-surface information have been compiled. Using these datasets, new stratigraphic correlations have been made on cross-sections delineating each Paleogene–Quaternary stratigraphic unit. The stratigraphic correlations enabled the construction of a 3D geological model using RockWorks and Viewlog, which illustrates the thickness and extent of regionally mappable (1: 100 000 scale) stratigraphic units. These stratigraphic units (SU) include gravel deposits constrained to benchlands (SU1) or plains (SU2); sand or gravel restricted to buried valleys and discrete meltwater channels (SU3); diamict of a wide grain-size range and distributed across much of the study area from both Cordilleran and Laurentide glaciations (SU4a); fine-grained diamict, silt and clay, or other fine-grained sediments associated with deposition in major glacial lakes (SU4b); and sand or gravel confined to modern valleys, glaciofluvial drainage-paths, and eolian deposits (SU5). This report describes the methodology used to develop the 3D model, provides insight on the key characteristics and depositional history of the selected stratigraphic units for which the Paleogene–Quaternary sediment thickness is classified and modelled, and shows the 3D distribution of the stratigraphic units through a series of maps (also released as a digital dataset), which can provide information needed to support land-use planning and resource management decisions in the shallow subsurface.

# 1 Introduction

Geological processes active during the Paleogene–Quaternary periods have deposited varied sequences of sediments in west-central Alberta. The Paleogene–Quaternary succession has been described through stratigraphic studies and surficial mapping (Roed, 1975; Catto et al., 1996; Utting, 2012, 2013; Atkinson and Pawley, 2013; Pawley and Atkinson, 2013; Atkinson et al., 2016; Utting et al., 2016). However, although the extent and morphogenesis of surficial deposits across west-central Alberta is well understood, the subsurface architecture of these units has only been defined at outcrops (Roed, 1968). These studies are important in understanding the geological history of the region, but they do not satisfy the requirements for a geological framework model that explicitly delineates the geometry and stratigraphic relationships of regional stratigraphic units.

A geological framework is important in west-central Alberta because it helps us better understand the subsurface architecture of shallow rock systems that are used to supply groundwater to industry, particularly in the exploitation of liquids-rich shale gas plays, which requires large quantities of water for multistage hydraulic fracturing of horizontal wells (Alberta Environment and Parks, 2006; Bruce et al., 2009; Johnson and Johnson, 2012; Rivard et al., 2014). To meet growing water demands, an examination of potentially water-bearing sediments in west-central Alberta is pertinent because relatively little is known about the geometry, lateral extent, and hydrogeological significance of Paleogene–Quaternary units, despite the rapid development of numerous industrial activities in the shallow subsurface.

Delineation of the geometry of Paleogene–Quaternary stratigraphic units is achieved in this study through 3D geological modelling of multisource surface and subsurface data. This report describes the methodology used to develop the 3D model, provides insight on the key characteristics and depositional history of the informal Paleogene–Quaternary stratigraphic units, and, through a series of maps, shows the 3D distribution of stratigraphic units, which may influence regional groundwater movement and surface water drainage systems. Specific objectives of this investigation are to synthesize available subsurface data to create lithological and stratigraphic databases; analyze sediment characteristics from outcrops and boreholes, framed within the conceptual geological history of the region, for unit correlation on cross-section; and to integrate units into a 3D geological model. The 3D reconstructions of sediment geometry presented in this report will be integrated into a regional geological and hydrogeological investigation of the area (Smerdon et al., 2016).

## 2 Study Area Characteristics

The study area encompasses 22 170 km<sup>2</sup> of west-central Alberta herein referred to as WCAB (Figure 1). WCAB includes the Town of Fox Creek, with the larger municipalities of Hinton, Edson, and Whitecourt located to the south and east of the study area. Although WCAB is largely unpopulated, with approximately 94% of the study area classified as Green Area (the forested portion of public land), the landscape contains widespread industrial infrastructure including oil and gas processing and storage facilities, gravel pits, well pads, pipelines, earthen dams, and gravel roads.

### 2.1 Physiography

WCAB is located at the western edge of the interior plains (Bostock, 1970). The southwest boundary of the study area is marked by the deformation front of the Rocky Mountain Foothills, with the remaining boundaries defined by drainage sub-basin divides. The physiography of the study area comprises three major elements: benchlands, the Swan Hills, and plains (Pettapiece, 1986; Figure 2). The benchlands have a step-form character and extend across the southwest half of the study area. They are highest in the southwest (up to 1600 m asl at the summit of Obed Mountain) and descend towards the northeast.

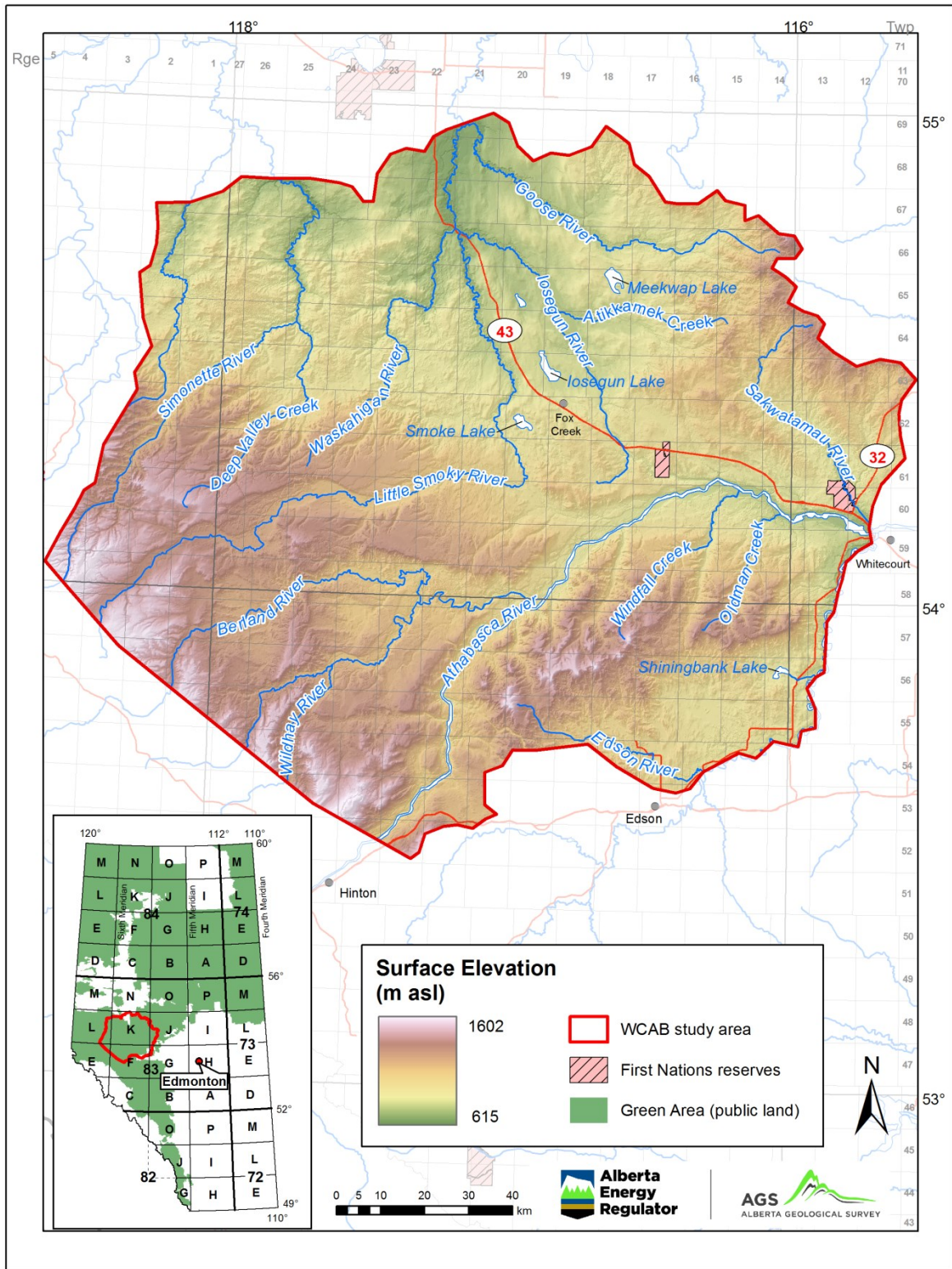
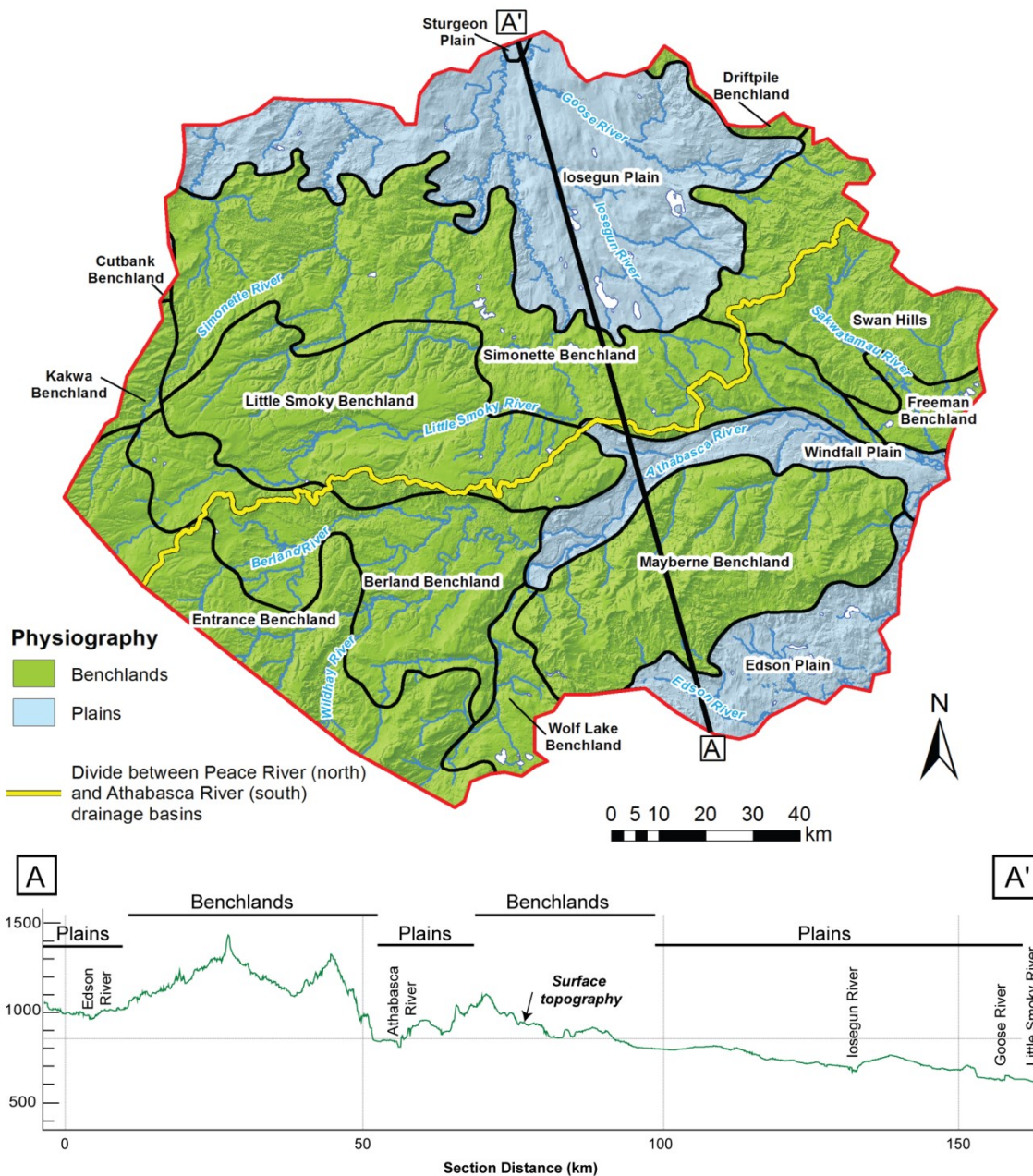


Figure 1. A hill-shaded digital elevation model (DEM) of the land surface in the study area showing major geographic features referred to in the text. Inset: map of Alberta showing the study area, Green Area, and NTS grid.



**Figure 2. Physiographic districts (from Pettapiece, 1986) and major drainage basins. Cross-section A-A' displays the surface topography of benchlands and plains. Cross-section is 30× vertically exaggerated.**

Relief within the benchlands is high. Steep slopes intervene between relatively flat steps, and river channels throughout the benchlands are deeply incised and have steep valley walls (cross-section A-A'; Figure 2). The flat summit of the Swan Hills (1350 m asl) lies immediately east of the study area. However, the rugged topography of its western flank comprises much of the northeastern corner of the study area. The benchlands and Swan Hills separate the Edson, Windfall, and the Iosegun plains (Pettapiece, 1986; Figure 2), which are characterized by low-relief terrain incised by shallow river channels (cross-section A-A'; Figure 2). These three major physiographic elements broadly reflect the

underlying bedrock surface in both elevation and relief (discussed further in Section 5). The benchlands and the Swan Hills form the main drainage divides separating the Peace and Athabasca river drainage basins (Figure 2).

### **3 Geological Background**

#### **3.1 Upper Cretaceous–Paleogene Bedrock Geology**

WCAB is underlain by a heterogeneous assemblage of continental fluvial and lacustrine sediments. The upper Cretaceous–Paleogene bedrock strata include three formations that subcrop at the bedrock topography surface as well as one unit that is buried below. From oldest to youngest these are the Wapiti (Chu, 1978; Dawson et al., 1994a; Fanti and Catuneanu, 2009), Battle (Irish, 1970; Hathway, 2011), Scollard (Gibson, 1977), and Paskapoo (Demchuk and Hills, 1991; Lerbekmo and Sweet, 2008) formations. These units were deposited by fluvial systems emanating from the mountain front during late-stage folding and thrusting of the Laramide orogeny. These fluvial systems deposited sands across the emerging foreland as well as fine-grained sediments deposited in lacustrine basins oriented parallel to the foothills (Dawson et al., 1994b). The Paskapoo Formation has the most extensive subcrop, underlying approximately 75% of WCAB (see Prior et al., 2013; Figure 3). This unit is partitioned into three members, with the uppermost sandstone-rich member (lithostratigraphically the Dalehurst Member of Demchuk and Hills, 1991, and hydrostratigraphically the Sunchild aquifer of Lyster and Andriashek, 2012) underpinning the high-elevation and high-relief benchlands and Swan Hills physiographic districts of WCAB (Figures 2 and 3; Section 2.1). The remainder of the Paskapoo Formation in WCAB is composed of the Lacombe Member, which consists primarily of siltstone and mudstone and is generally present in the plains (Figure 2), and potentially small portions of the sandstone-rich Haynes Member (Lyster and Andriashek, 2012). All bedrock units have eastward-thinning wedge-shape geometry as a result of both tectonic deformation of the basin during the late-stages of the Laramide orogeny and the extensive removal of sediment during post-Laramide erosion (cf. Figure 4 in Lyster and Andriashek, 2012). The Scollard, Battle, and Wapiti formations directly underlie the Paskapoo Formation and only subcrop where the Paskapoo Formation has been eroded, with older bedrock units progressively subcropping towards the north (cross-section A-A'; Figure 3). These units are unconformably overlain by Paleogene–Quaternary fluvial and glaciogenic sediments.

#### **3.2 Paleogene–Quaternary Geology**

##### **3.2.1 Preglacial Geological History**

The preglacial history of the study area was dominated by fluvial incision and planation of the bedrock surface that produced a step-like landscape architecture in which younger planation surfaces are positioned topographically at lower elevations than older planation surfaces (cf. Alden, 1932; Vonhof, 1969; Edwards and Scafe, 1996; Leckie, 2006). Collectively, Roed (1968, 1975), St-Onge (1972), and Edwards and Scafe (1996) identified four gravel-capped fluvial planation surfaces within the study area:

- the Swan Hills, Entrance, and Mayberne benchlands;
- the Berland, Little Smoky, and Simonette benchlands;
- the Edson, Windfall, and Iosegun plains; and
- paleovalleys.

Although the age of the higher elevation surfaces remains uncertain, basal gravels within paleovalleys are inferred to have been deposited during the mid-Wisconsinan, since they occupy the same stratigraphic and topographic position as correlative deposits within the infill sequence of the Smoky and Peace rivers

(Westgate et al., 1971, 1972; Liverman, 1989; Liverman et al., 1989; Catto et al., 1996; Morgan et al., 2012).

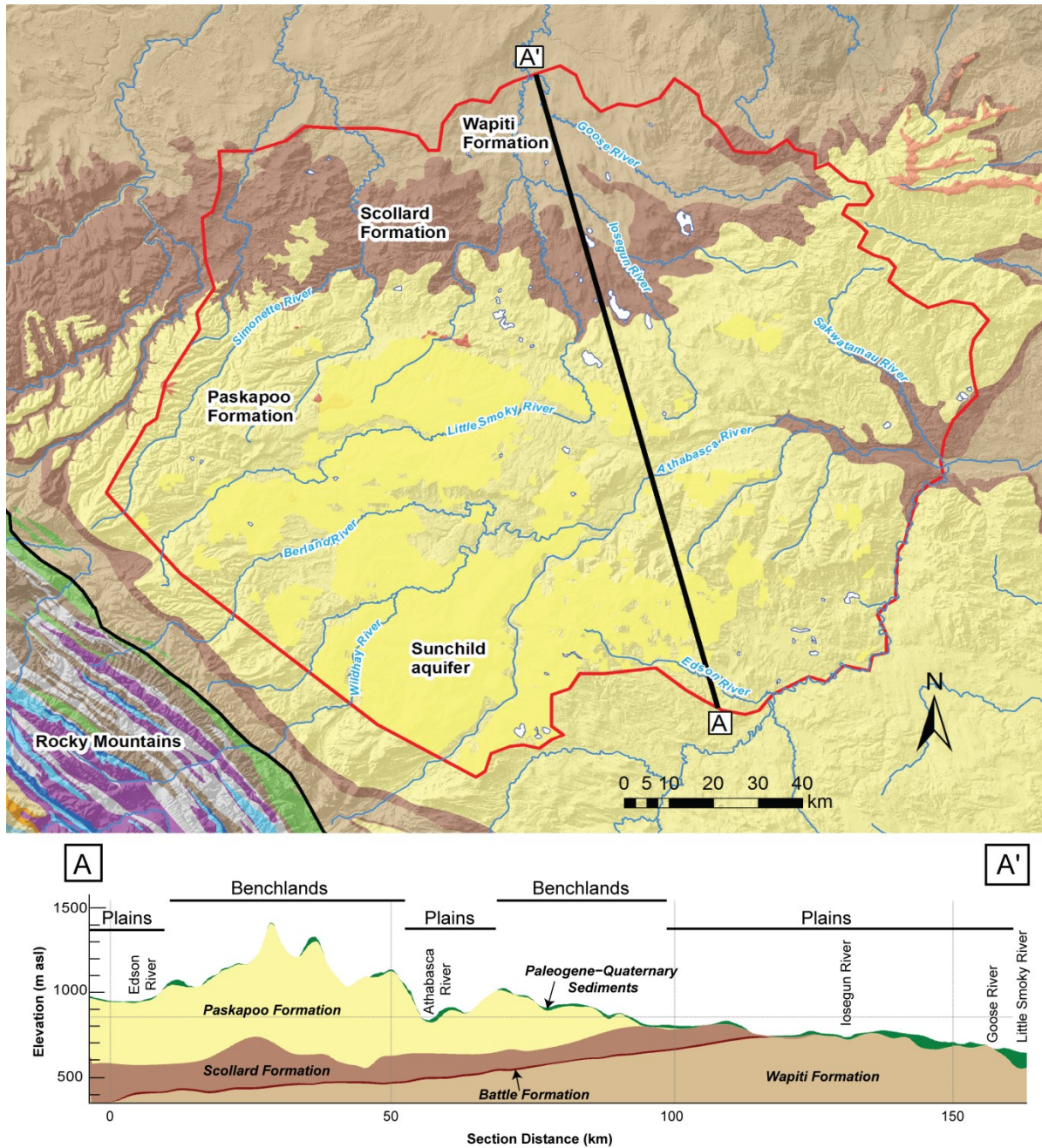


**Figure 3. Bedrock geology map of WCAB and adjacent areas (modified from Prior et al., 2013). The extent of the Sunchild aquifer is overlain (solid pale yellow; Lyster and Andriashek, 2012). Cross-section A-A' illustrates the wedge-shaped geometry of bedrock units and their relationship with the physiographic regions in the study area. Cross-section is 30× vertically exaggerated.**

### 3.2.2 Laurentide-Cordilleran Glacial Geological History

During the Late Wisconsinan, the Cordilleran and Laurentide ice sheets subsumed the study area, coalescing along a spatially and temporally transgressive, southeast-oriented suture zone (Figure 4). Glacially streamlined, lithologically distinctive sediments relating to these ice sheet expansions record the pattern and relative timing of advance, convergence, and retreat of both ice sheets (Roed, 1968, 1975; Andriashek, 2001; Atkinson et al., 2016; Utting et al., 2016).

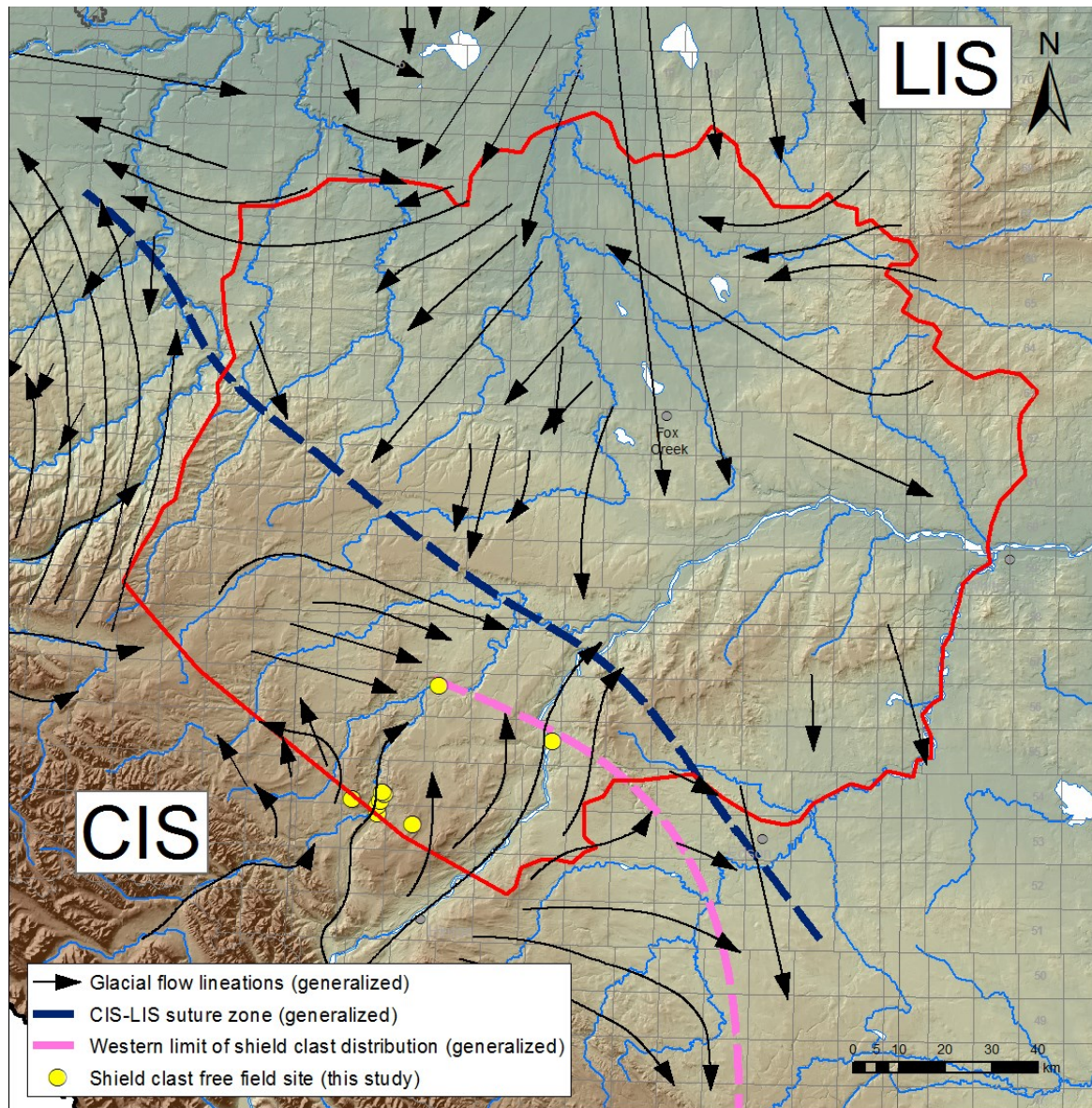


**Figure 4. Generalized Cordilleran Ice Sheet (CIS) and Laurentide Ice Sheet (LIS) glacial flow lineations and suture zone (modified from Roed, 1968, and Atkinson et al., 2016). Western limit of shield-clast distribution modified from Roed (1968) based on field observation.**

The initial advance of both the Cordilleran Ice Sheet and Laurentide Ice Sheet were topographically unconstrained and included convergence to the east of the foothills and mutual deflection of flow. Subsequently, strengthened southwest flow of the Laurentide Ice Sheet displaced the Cordilleran Ice

Sheet by up to 60 km to the eastern foothills (Atkinson et al., 2016). The limit of Laurentide Ice Sheet extent in the study area coincides with a lithological boundary between surficial sediments with and without Laurentide-provenance material (distinctive pink granite and granite gneiss) in the foothills (Figure 4; Roed, 1968, 1975; Andriashek, 2001; Atkinson et al., 2016). During this phase, Cordilleran Ice Sheet flow from trunk valleys was deflected southward and converged with the Laurentide Ice Sheet in a narrow zone parallel to the mountain front. The mutually deflected flow extended to the Canada–U.S. border and emplaced the foothills erratic train (distinctive quartzite erratics that occur in the Athabasca Valley and along the foothills as far as the international border; Stalker, 1956; Gravenor and Bayrock, 1961; Roed, 1975; Levson and Rutter, 1996; Atkinson et al., 2016; Utting et al., 2016). The terminus of this flow represents the all-time maximum southwestern extent of the Laurentide Ice Sheet (Jackson et al., 1997, 1999).

Deglaciation proceeded via desuturing of the ice sheets from south to north (Atkinson et al., 2016; Utting et al., 2016). Initial retreat of the Laurentide Ice Sheet de-buttressed the Cordilleran Ice Sheet, facilitating the eastward expansion of a series of valley and piedmont glaciers onto the plains (Roed, 1968, 1975; Atkinson et al., 2016). The continued northeast retreat of the Laurentide Ice Sheet from WCAB proceeded down the regional slope of the plains. Consequently, glacial lakes impounded against the Laurentide Ice Sheet resulting in the accumulation of glaciolacustrine sediment. These decanted through a series of successively lower basins as new outlets were exposed upon ice retreat (St. Onge, 1972; Utting et al., 2015, 2016). The most significant glacial lake basins within the study area include that of Glacial Lake Miette, Glacial Lake Edson, and Glacial Lake Iosegun (e.g., glaciolacustrine deposits; Figure 5; St. Onge, 1972; Utting et al., 2015, 2016).

Roed (1968, 1975) and Utting et al. (2016) suggested that the Cordilleran Ice Sheet may have extended onto the plains before the Late Wisconsinan. However, no deposits relating to this advance have been mapped in WCAB. The well-documented stratigraphies at Watino and Simonette (Westgate et al., 1971, 1972; Liverman et al., 1989; Catto et al., 1996), which are nearer the ice-dispersal centres of the Laurentide Ice Sheet (Dyke et al., 2002) than the study area, indicate that all Laurentide glaciogenic units identified in this study are Late Wisconsinan.

## 4 Methodology

Using the Paleogene–Quaternary geological history as a conceptual guide, a 3D geological model of the unconsolidated deposits was developed through combining a lithological database of multisource borehole and field data, geospatial datasets in GIS format, and published gridded-surface information. Field data were collected to check the accuracy of nearby subsurface information compiled in the lithological database and to add control points in areas of sparse subsurface data or poorly constrained bedrock topography data. Combining these datasets allowed for analysis in cross-section format, the outcome of which was used to create an updated grid of the modelled bedrock topography and to determine regionally significant Paleogene–Quaternary stratigraphic units. Computer modelling of correlated borehole data on cross-section was used to build a 3D model in which the component parts illustrate the location, lateral extent, and thickness of Paleogene–Quaternary stratigraphic units.

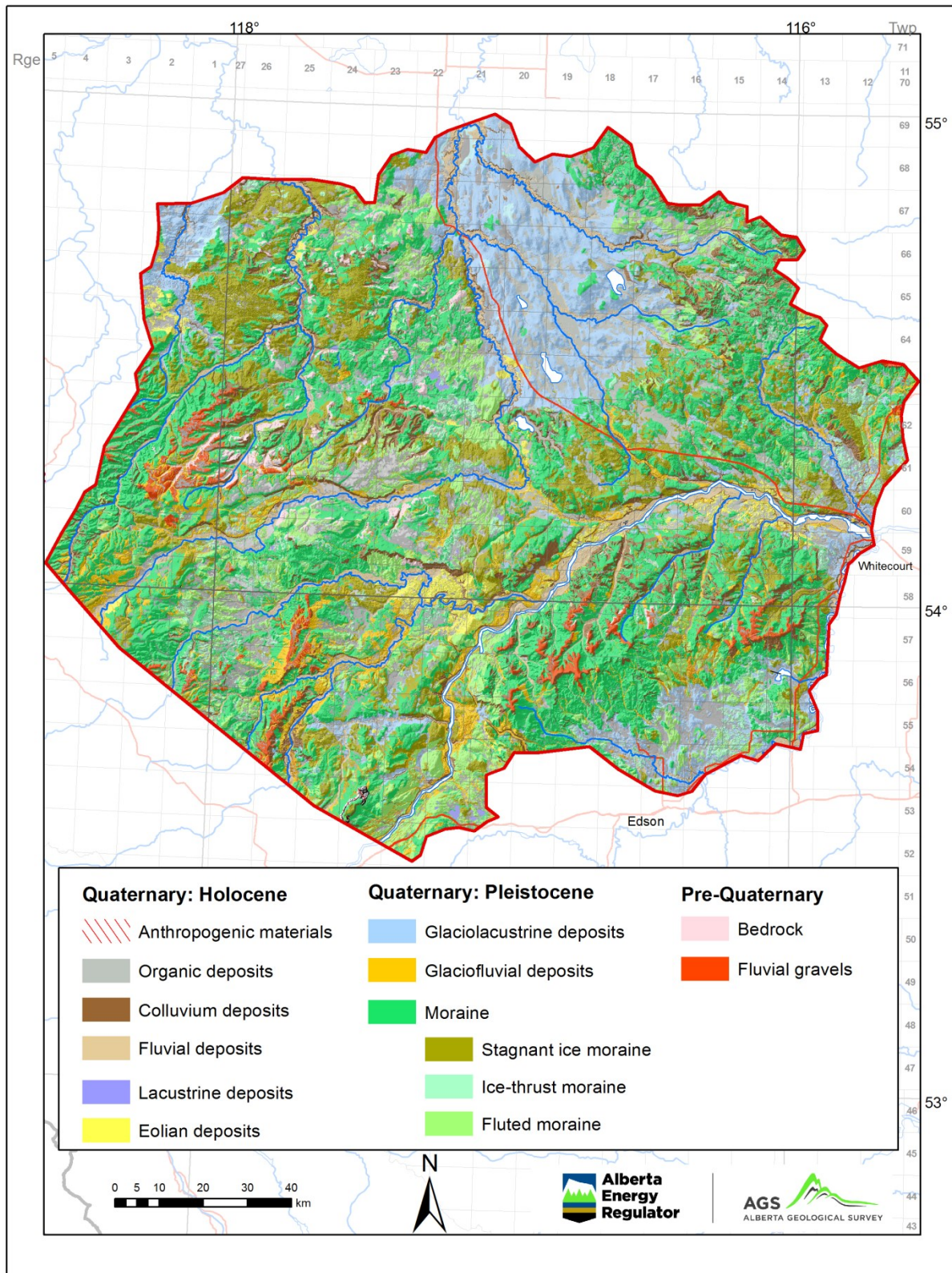


Figure 5. Surficial geology map of WCAB and adjacent areas (from Atkinson et al., 2017).

## 4.1 Lithological Database

A database of subsurface information was created to integrate original lithological information from boreholes and field sites. This database includes publicly available water-well information from the Alberta Water Well Information Database (AWWID; AEP, 2015) and other multisource data. Although the AWWID has the most extensive coverage of lithological data throughout the study area (Figure 6a), it is generally considered to be of variable-to-low quality due to nonstandardized lithological descriptions. The following higher quality data was used for this study: three wet-rotary boreholes logged by Alberta Geological Survey (AGS) staff to depths between 120 m and 151 m (Smerdon et al., 2016); data from the Groundwater Observation Well Network collected by AEP; geophysical logs (resistivity and spontaneous potential) collected by the Alberta Research Council (ARC) coal surveys; mineral industry core, which was used for identifying the top of bedrock; and lithological information from aggregate pits (Figure 6a). Interpreted contour data from previous studies were also incorporated into the lithological database to help inform the modelling of the updated bedrock topography surface (see Section 5).

### 4.1.1 Calibration of Variable Quality Data with Field Observations

Because the database is composed mostly of AWWID lithologs, a field program was undertaken to calibrate these records with section logs and fill in areas where data were sparse. Data points collected as part of this field program also aided in refining the bedrock topography (discussed in Section 5) and informing the selection of Paleogene–Quaternary stratigraphic units (discussed in Section 6). Ground-based investigations were conducted at accessible outcrops, and helicopter surveys were done to examine outcrops along remote rivers (Figure 6b). Field data from 505 sites collected during AGS surficial geology mapping in the region were also compiled in the lithological database. These data describe the lithology of the upper 1–3 m of sediments, as well as grain-size analyses taken from 44 field locations. In total, 166 new field observations were collected in this study (the locations are shown in Figure 6b).

## 4.2 Cross-Section Analysis and Model Construction

Lithological data were plotted in cross-section using Viewlog because it is able to easily import multisource data and to dynamically display cross-sections together with plan view maps of GIS information. A 12 m resolution digital elevation model (DEM; from Sustainable Resource Development) of the land surface topography was resampled to 200 m (the cell size of this study) and posted, along with other available gridded data (e.g., the provincial-scale bedrock topography), on cross-sections to show the relationship of topographic surfaces to subsurface data. Compiling this information into one software platform facilitated the correlation of laterally extensive stratigraphic units and the bedrock topography.

The Paleogene–Quaternary stratigraphic units and the bedrock topography were modelled using different methodologies than those available in Viewlog. Pick assignments correlated in Viewlog were imported into Esri ArcMap to interpolate the bedrock topography and RockWorks to model the stratigraphic units.

### 4.2.1 Bedrock Topography Modelling

A total of 17 990 data points from multisource borehole data, as well as interpreted synthetic contour information (Section 5), were used to generate the revised modelled surface of the bedrock topography (Figure 7). Ordinary kriging in the Geostatistical Analyst extension in Esri ArcMap was used to construct the initial surface. Grid math was then used to truncate the bedrock topography surface by the resampled DEM of the land surface topography (200 m grid cell size) where the two intersected to ensure that the bedrock topography surface never exceeded the land surface at any given location. This is particularly relevant where incision by present-day rivers expose the underlying bedrock strata.

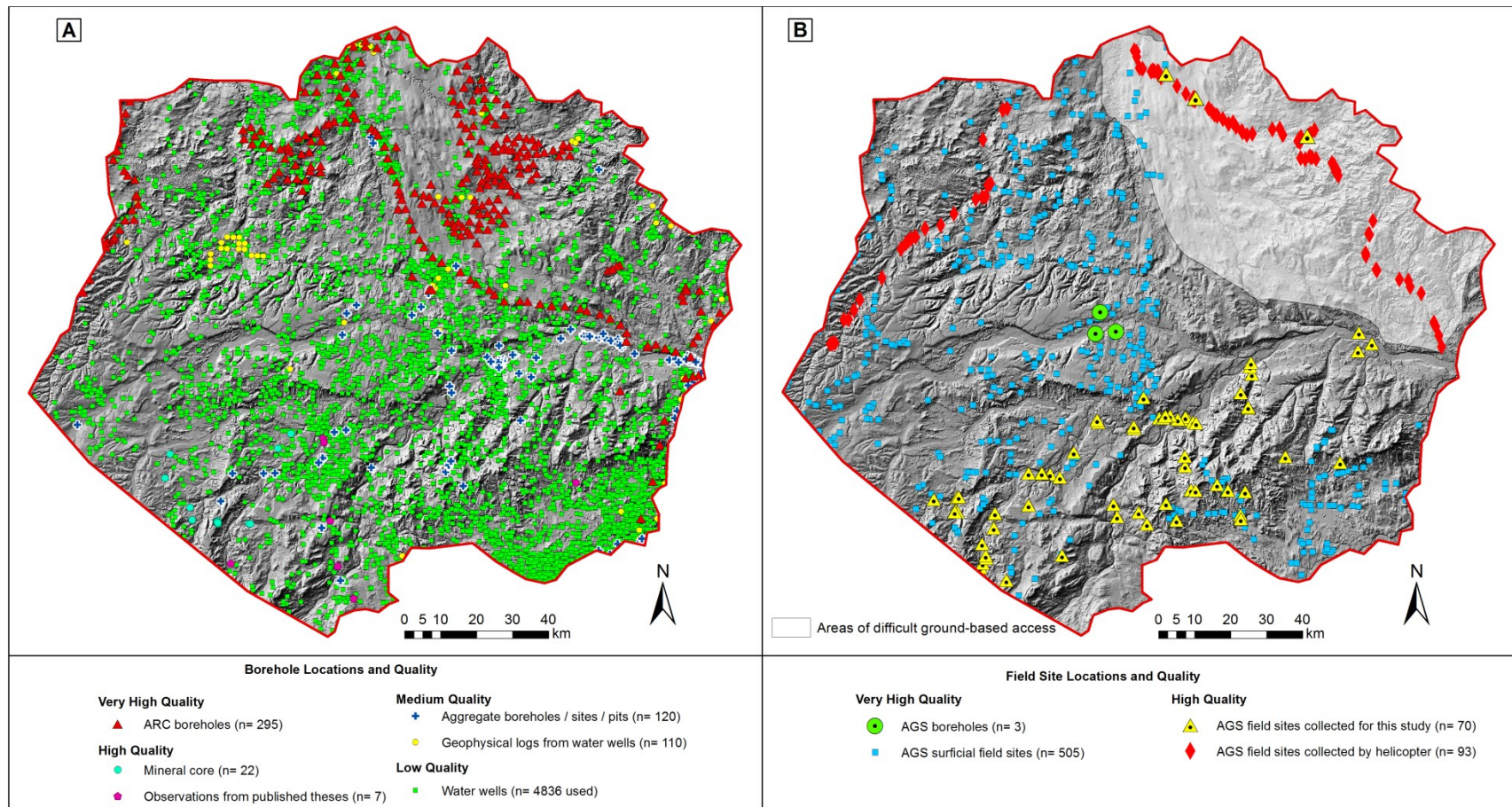


**Figure 6. Hill-shaded bare-earth LiDAR DEM showing locations of (a) borehole data compiled in the lithological database and (b) field data collected by the AGS. Data quality ranges from high to very high (collected by AGS, industry, and academia), medium (collected by industry or multisource borehole data with geophysical logs but unverified location information) and low to variable (compiled in the AWWID).**

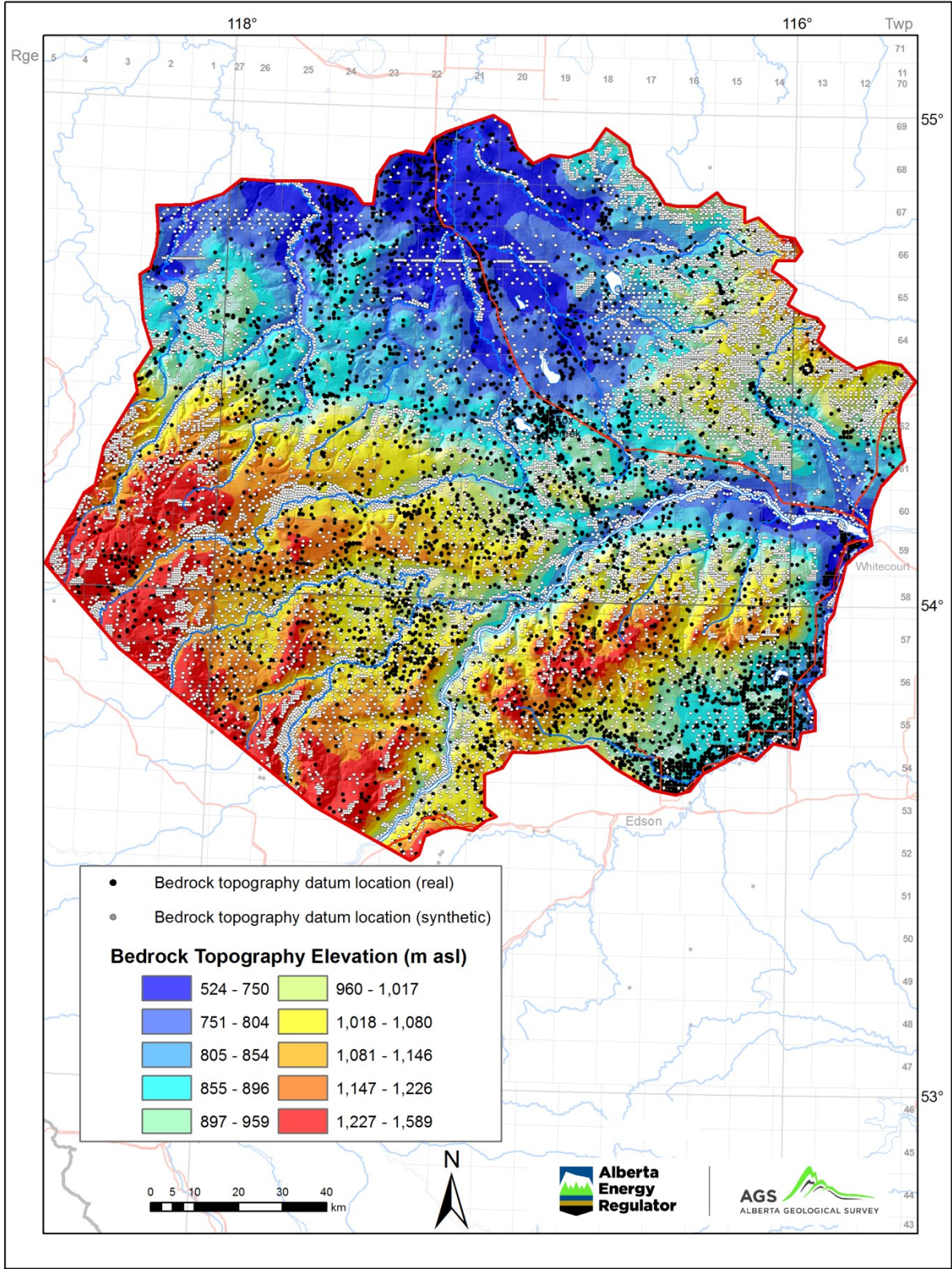


Figure 7. A digital elevation model (DEM) of the bedrock topography of the study area and location of input data.

#### **4.2.2 Paleogene–Quaternary Stratigraphic Unit Modelling**

Using the modelled bedrock topography surface as a base, a total of 5946 stratigraphic picks of Paleogene–Quaternary stratigraphic units were imported into RockWorks to create the 3D stratigraphic model. Inverse distance weighting (IDW<sup>2</sup>) with a minimum search radius of eight points was used to interpolate stratigraphic picks and synthetic data to create top and base surfaces for each stratigraphic unit. Limited synthetic data in the form of surficial map polygons (from Fenton et al., 2013) was used to help constrain the distribution of modern fluvial sediments (SU5; see Section 6.5) because available borehole data was limited in these locations. Following interpolation, the model was built from the base up to ensure that onlapping of units occurred with no unit cross-overs (i.e., did not violate geospatial and temporal relationships). The geometry and extent of each stratigraphic unit modelled surface was then constrained by the unconformable bounding surfaces of the bedrock topography and present-day land surface.

### **5 Bedrock Topography and Sediment Thickness**

The stratigraphic framework of the Paleogene–Quaternary strata presented in this report includes major mappable stratigraphic units, the base of which is defined by the bedrock surface (Figure 7). The bedrock topography in WCAB has been mapped at a regional scale by Gabert and Roed (1968) and Carlson and Green (1979) and has been digitally rendered at a provincial scale most recently by MacCormack et al. (2015). However, the high relief of the bedrock topography within WCAB, and its importance for modelling the thickness, distribution, and architecture of overlying Paleogene–Quaternary stratigraphic units required that it be rendered with greater resolution than that provided by the provincial-scale model. Four types of data were used to evaluate the bedrock topography in WCAB: (1) newly collected field data (Section 4.1.1) and borehole interpretations; (2) interpreted contour and point data used in the provincial-scale model (MacCormack et al., 2015); (3) point data from surficial mapping projects (Utting, 2012, 2013; Fenton et al., 2013; Atkinson and Pawley, 2013; Pawley and Atkinson, 2013); and (4) synthetic points (Figure 7). Interpreted contour and point data used in the provincial-scale model were re-evaluated and compared on cross-section with available subsurface data. Synthetic points were created to constrain the bedrock surface where data were sparse or the complexity of the bedrock topography required further control points to influence the geometry of the modelled surface. The updated bedrock topography of WCAB is presented in Figures 7 and 8a. The sediment thickness map (Figure 8b) is a derivative created by subtracting the elevation of the bedrock surface from that of the land surface DEM (Figure 1).

The bedrock surface descends over 1000 m from the southern benchlands and flanks of the Swan Hills (~1590 m asl) to the plains in the north (525 m asl; Figures 2 and 7). Sediment is relatively thin where the bedrock surface is high and thicker where it is low. Benchlands in the western parts of the study area are mantled by the thinnest deposits (typically 0–5 m; Figure 8b) while the Iosegun and Windfall plains are mantled by relatively thick sediment (typically 25 m to approximately 40 m; Figure 8b). Locally, discontinuous deposits of thick sediment (approximately 25 m) are perched along the walls of deeply incised bedrock valleys in the benchlands. These deposits are interpreted as paleovalley infill and are discussed further in Section 6.2. Paleovalley thalwegs are shown on Figures 8 and 13.

The physiography of the modern land surface largely reflects the underlying form of the bedrock topography. In the high-elevation, high-relief benchlands and Swan Hills, bedrock is correspondingly high and rugged, whereas in the plains, bedrock has a subdued relief. The stepped physiography of the benchlands and deeply incised valleys, and the rugged relief of the western Swan Hills, relate to the character of the underlying bedrock that has not been masked by overlying sediment. In contrast, any bedrock features underlying the plains are obscured by relatively thick (approximately 25 m; Figure 8b) sediment. Prominent features on the bedrock surface (and correspondingly the land surface physiography)

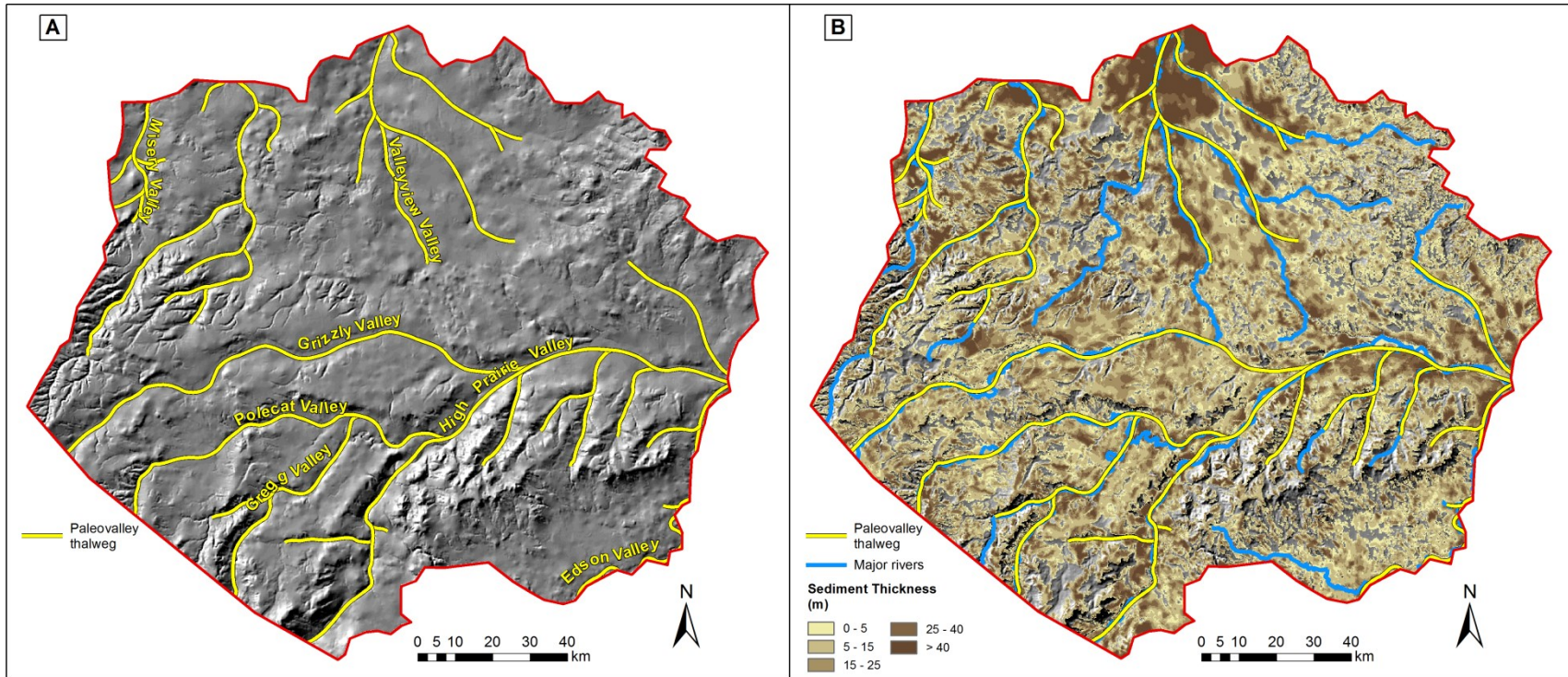


Figure 8. (a) A hill-shaded DEM of the WCAB bedrock topography showing paleovalley thalwegs (modified from Lennox, 1966; Carlson and Green, 1979; Balzer, 2000; MacCormack et al., 2015). Paleovalley names including Edson, High Prairie, and Valleyview valleys from Lennox (1966); Carlson and Green (1979); and Balzer (2000). Misery, Grizzly, Polecat, and Gregg valleys are named here for local geographic features, following Geiger (1965). (b) Sediment thickness map of the Paleogene–Quaternary succession. Areas of 0 m sediment thickness are shown where the underlying hill-shaded DEM (grey-scale) is exposed. Paleovalley thalwegs are also shown.

typically coincide with the distribution of the Paskapoo Formation (Figures 2 and 3), likely because it is more resistant to erosion than the Scollard, Battle, and Wapiti formations (discussed in Section 3.1) that underlie the plains.

Physiographic interpretation of the bedrock topography and modern land surfaces (Figures 1 and 7) coupled with an understanding of the geological history of the study area (Section 3.2) provide important context for stratigraphic interpretation of Paleogene–Quaternary deposits. Different suites of sediments are expected to occupy different physiographic settings. For example, benchland planation surfaces are typically mantled by thin sediment cover composed of gravel (where preserved) or diamict (till), while buried valleys are typically infilled with a thick sediment package composed of gravel at the base, finer valley infill sediment, and diamict (till) at surface. The significance of the modern land surface and bedrock topography physiographic settings is discussed, where applicable, in Section 6.

## 6 Paleogene–Quaternary Stratigraphy

Paleogene–Quaternary deposits have been classified into informal stratigraphic units based on lithology, stratigraphic and topographic position (relative to both the bedrock topography and the modern land surface), genesis, and depositional setting. These sediments are classed into mappable stratigraphic units (Figure 9; Table 1) and rendered at a regional scale (1:100 000). Units that are recognized locally but are not mappable at the scale of this study were identified on cross-section but not incorporated into the final 3D model.

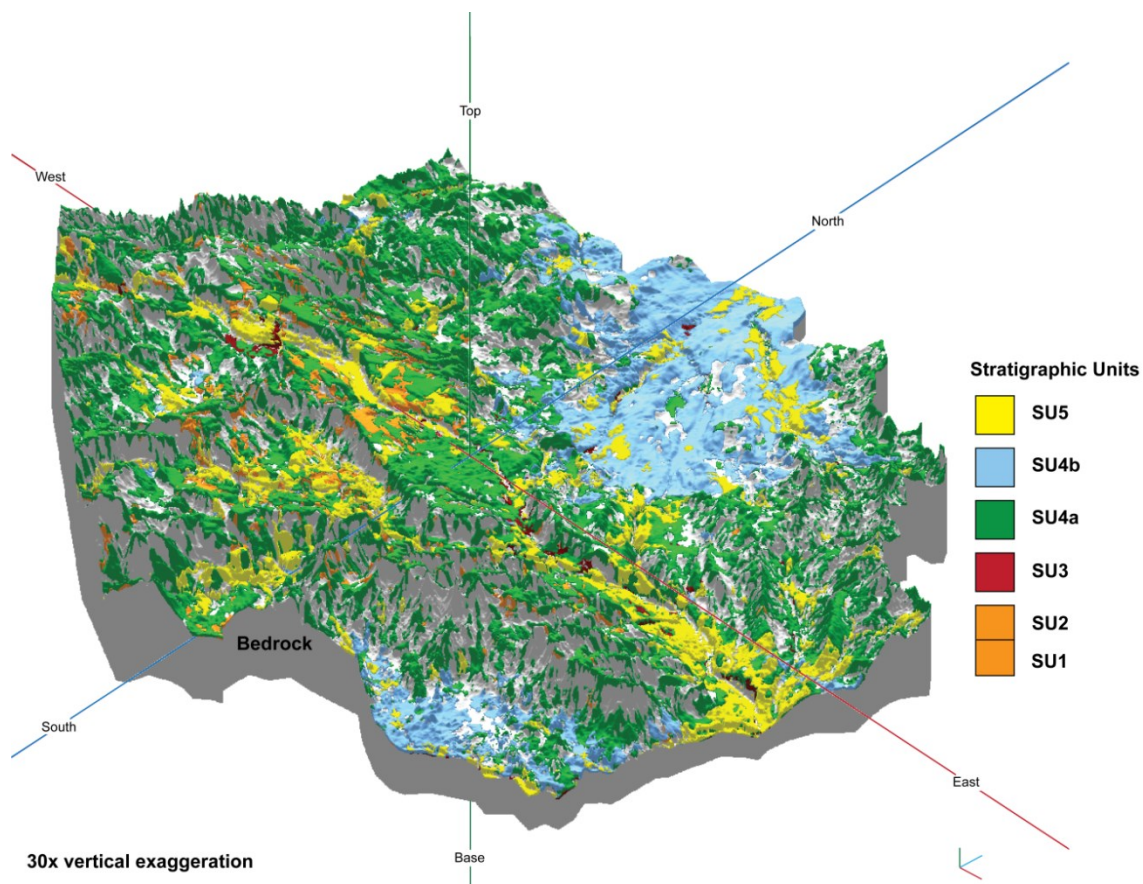


**Figure 9. 3D view of modelled Paleogene–Quaternary stratigraphic units overlying bedrock. Characteristics of units are described in Table 1.**

**Table 1. Sediment characteristics and model summary statistics of Paleogene–Quaternary stratigraphic units.**

| Stratigraphic Unit (SU) | Mappable (regional scale) | Unit Description   | Modelled Volume (%) |
|-------------------------|---------------------------|--|---------------------|
| Organics                | No                        | Peat and other organic accumulations at land surface.  | n/a                 |
| SU5                     | Yes                       | Fluvial, glaciofluvial, sand and gravel, or eolian sand.   | 14.25               |
| SU4b                    | Yes                       | Fine-grain diamict, silt and clay, or glacially disturbed bedrock; deposited or reworked by glacial sources and/or glaciolacustrine processes. | 27.85               |
| Sand interbeds          | No                        | Discrete sand (or stratified sediment) beds within SU4b and/or SU4a; sand beds separating SU4b and SU4a.                                       | n/a                 |
| SU4a                    | Yes                       | Diamict (varied grain size); silt and clay; glacially reworked or displaced bedrock.   | 48.08               |
| SU3                     | Yes                       | Sand and/or gravel resting on the floors of bedrock valleys.   | 3.11                |
| SU2                     | No; included with SU1     | Sporadically distributed gravel included with SU1; unit underlies glaciogenic sediments and overlies bedrock on discrete plains.               | n/a                 |
| SU1                     | Yes                       | Gravel directly overlying bedrock on step-form benchlands.   | 6.71                |
| Bedrock                 | Yes                       | Top of bedrock strata, comprising outcrops of the Paskapoo, Scollard, Battle and Wapiti formations.  | n/a                 |

## 6.1 SU1/SU2: Gravel Overlying Bedrock on Benchlands and Plains

Coarse-deposits of SU1 and SU2 are combined into a single modelled unit because SU2 was present in only a small number of lithological descriptions from water wells. We chose to correlate SU2 on cross-section where possible and to combine the SU2 data with SU1 for ease of modelling.

Samples collected from AGS boreholes intersect SU1. This unit consists predominantly of massive- to crudely-bedded, clast- to matrix-supported pebble to boulder gravel (Figure 10). Lithologically, SU1 is dominated by quartzite and chert (AGS borehole WCAB-15-03; Figure 10), with minor sandstone, conglomerate, and ironstone (Edwards and Scafe, 1996). Limestone is notably absent from SU1, and the matrix is noncalcareous. SU1 is typically oxidized and is dark yellowish-brown to olive brown in colour. The contact between SU1 and an overlying stony diamict (correlated in some cases to SU4a) is often difficult to distinguish (Figure 10c) because both units are texturally similar (Table 2; Roed, 1968, 1975).

SU1 primarily mantles the step-form bedrock that underpins the benchlands (Figure 2) in the southwest part of the study area (Figures 10a and 11) and has a relatively uniform sediment isopach (Figures 10b and 12). The unit is typically overlain by coarse-grained diamict of SU4a (Table 1 and Figure 10c). Locally, SU1 may be overlain by thin surface deposits of glaciofluvial sand and gravel (SU5; Figure 9).

SU2 is a thin, laterally restricted gravel unit that is only identified on the Edson Plain (Figure 2). Although gravel on the plains has been noted by previous researchers (Lowland gravels; Roed, 1975), the unit was deemed unmappable at a regional scale (1:100 000). Despite being recognizable as a topographically lower deposit in subsurface datasets, SU2 was not considered as a discrete unit within the model and was instead combined with the texturally similar and regionally more extensive SU1.

SU1 is distributed across step-form benchlands that have been interpreted as the geomorphic product of fluvial incision and planation in which topographically lower steps are younger than higher steps

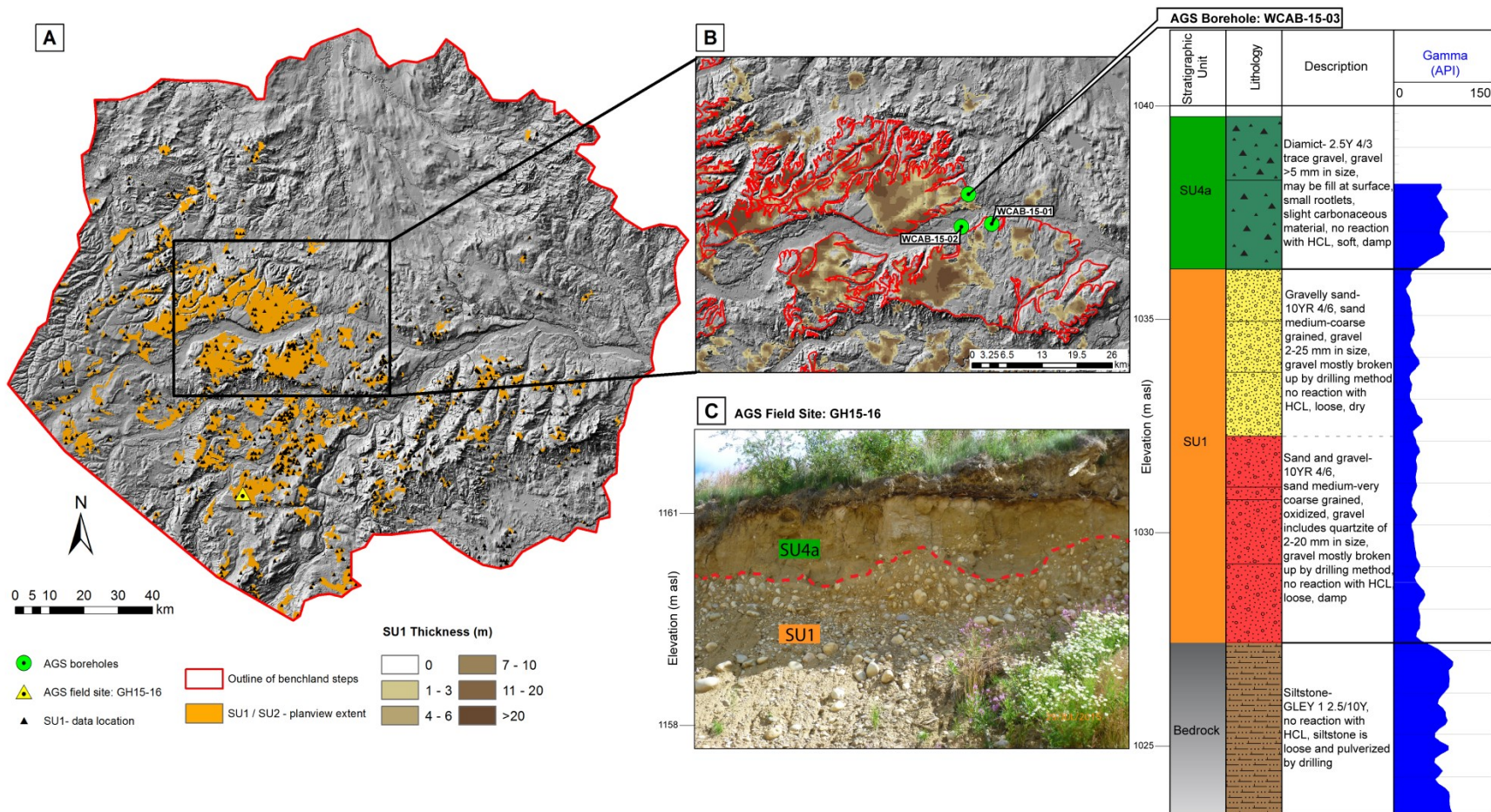


**Figure 10. (a) Hill-shaded bare-earth LiDAR DEM showing SU1/SU2 data locations and modelled extent. (b) Detailed view of the SU1 isopach across benchland steps (outlined in red) and the location of AGS boreholes. Lithological descriptions and gamma-ray log from AGS borehole WCAB-15-03 in which SU1 was identified. (c) Outcrop showing the contact of SU1 and SU4a, AGS field site GH15-16.**

**Table 2. Selected grain size results from SU1 and SU4a. Fraction above sand was not analyzed.**

| Stratigraphic Unit (SU) | Source                   | Site Identifier | Sand % | Silt % | Clay % | Lithological Description   |
|-------------------------|--------------------------|-----------------|--------|--------|--------|--|
| SU4a                    | AGS surficial field site | NA11-244        | 34.54  | 48.68  | 16.78  | Olive brown sandy silt diamict (till)  |
|                         | (Roed, 1975)             | 223             | 34.00  | 26.00  | 40.00  | Medium olive brown till; very plastic, slightly sandy, moderately stony  |
|                         | AGS surficial field site | SP11-154        | 28.17  | 40.58  | 31.25  | Greyish brown sandy silt till/diamict  |
|                         | AGS borehole             | AGS-WCAB-15-01  | 35.46  | 42.19  | 22.35  | Olive brown (2.5Y4/3); clay-sand-silt; pebbles (metaquartzite); coal fragments; some oxidized small pebbles; crumbly (dry); calcareous (strong reaction) |
| SU1                     | AGS surficial field site | NA11-218        | 42.15  | 40.58  | 17.27  | Olive brown sandy silt diamict   |
|                         | AGS surficial field site | SP11-226        | 54.5   | 31.93  | 13.57  | Light brown silty sand diamict   |
|                         | AGS surficial field site | SP11-228        | 84.82  | 11.16  | 4.02   | Yellowish-brown silty sand diamict   |

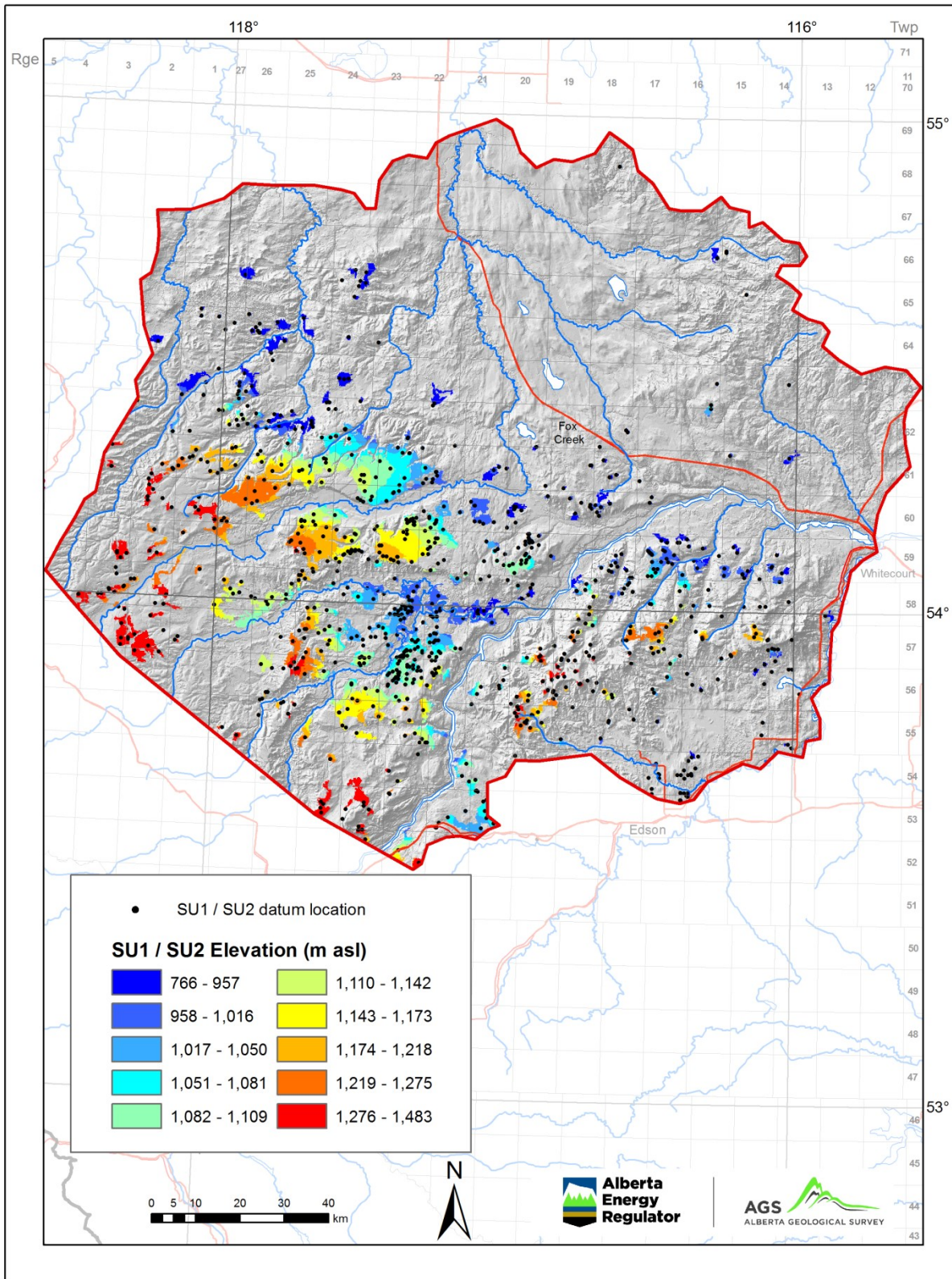


Figure 11. Hill-shaded bare-earth LiDAR DEM showing the elevation of SU1.

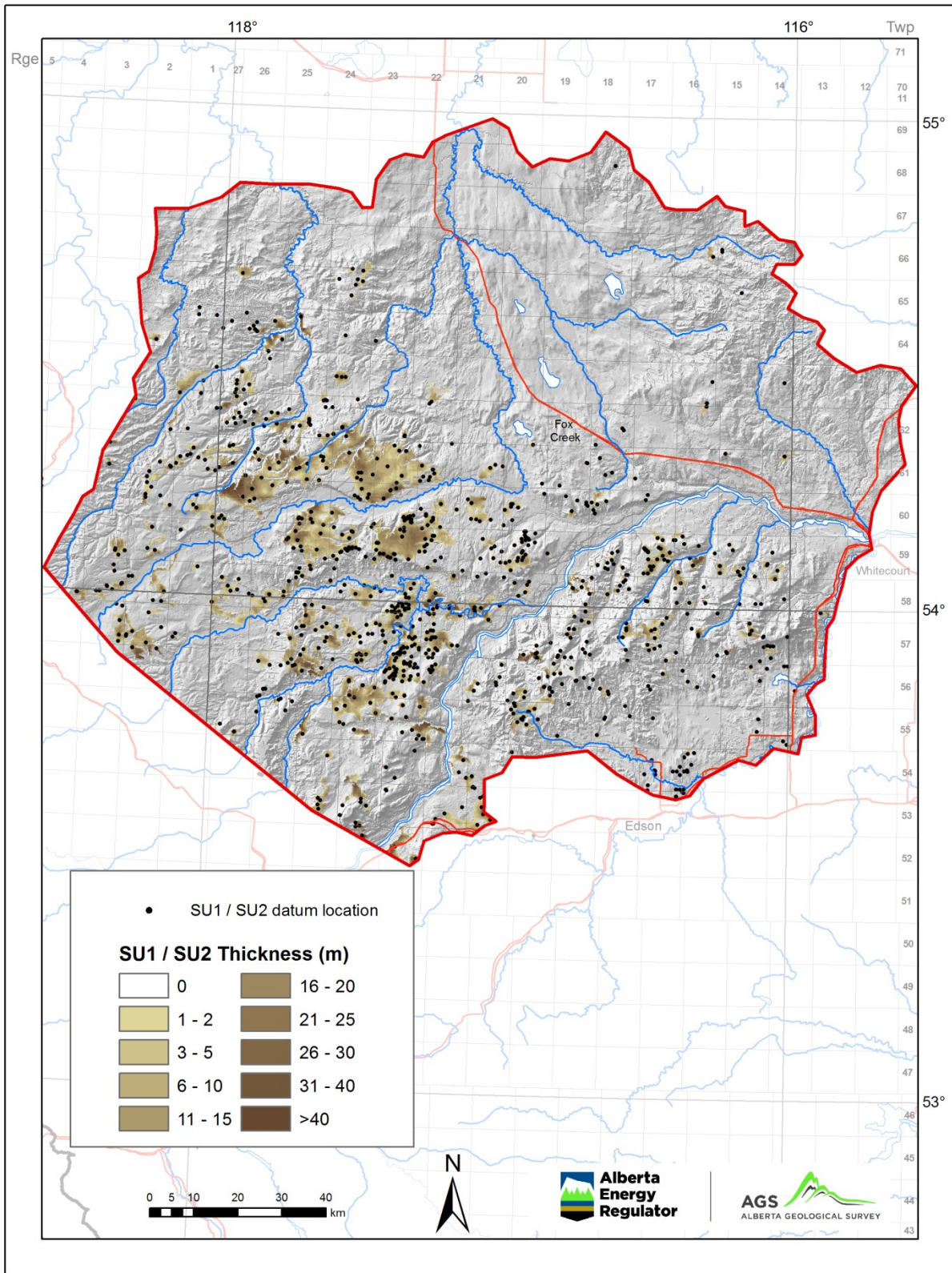


Figure 12. Hill-shaded bare-earth LiDAR DEM showing the thickness of SU1.

(Edwards and Scafe, 1996). The generally elevated position of the benchlands themselves, which presumably were valley bottoms at the time of deposition, is attributed to topographic inversion by differential erosion between soft sedimentary bedrock and the gravel unit itself, which is relatively resistant (Howard, 1960). The distribution and thickness of the unit reflects the extent of fluvial planation and deposition by major paleorivers within the study area. The absence of granitic or gneissic clasts derived from the Canadian Shield indicates that the fluvial component of SU1 predates Laurentide glaciation.

## **6.2 SU3: Buried-Valley Gravel Deposits**

SU3 is poorly exposed in the study area. Therefore, lithological descriptions for the unit are based on previous investigations by Carlson and Green (1979) and Edwards et al. (2006), as well as AWWID borehole descriptions. The unit consists of light olive-brown to light greyish-brown, poorly sorted, silty sand and gravel with clasts up to cobble-size. Lithologically, the sand is composed of quartz with some black chert, and the gravel is dominantly quartzite.

SU3 is defined by its confinement to the base of buried bedrock valleys and adjacent terraces (Figures 13 and 14). The unit is typically buried beneath fine-grained glaciogenic units (SU4a or SU4b; Table 1), except in major valleys of the benchlands (e.g., Little Smoky, Wildhay, and Athabasca rivers; Figure 1) where the unit is near surface. As a result of emplacement within valleys, SU3 has an elongate geometry that pinches out laterally at valley margins (cross-section B-B', Figures 13 and 15).

The close association between SU3 and buried valleys suggests that the majority of SU3 deposits were emplaced by fluvial processes confined within an incised drainage system that predates the last (Late Wisconsinan) glaciation (thalwegs; Figures 8 and 13; Roed, 1975). A lesser volume of SU3 may have been emplaced at the base of buried glacial meltwater channels, which are of limited lateral extent. Overlying units typically include clay- to silt-dominated sediment transitioning upward into a diamict. The fine-grained sediments are interpreted to have been deposited in proglacial lakes impounded within valleys by the advancing Laurentide Ice Sheet and are classed as SU4b. The diamict is interpreted as till (either SU4a or SU4b). However, the description of a transitioning-upward succession is not observable in all borehole records and is therefore not considered mappable in this study. In some cases, SU5 overlies or infills channels incised into SU3, especially within the benchlands where SU3 is not deeply buried (Figure 16). The contact between these texturally similar units was difficult to establish in borehole records (e.g., cross-section B-B', Figure 13). However, surficial maps segregate these units as fluvial (SU3) or glaciofluvial (SU5), which delimits the distribution of SU5 and its extent within the subsurface. The contact with underlying bedrock strata is unconformable, and no intervening sediments are positioned between SU3 and bedrock.

## **6.3 SU4a: Coarse-Grained Glaciogenic Diamict**

Glaciogenic sediments have been classified as SU4 and are texturally subdivided into coarse-grained diamict (SU4a) and silt to clay diamicts (SU4b).

SU4a is the most complex and texturally variable unit in WCAB. It consists dominantly of matrix-supported sand to silt diamict, with minor silt and clay. In cross-section, SU4a contains occasional rafts of glacially displaced bedrock, and lenses of stratified sediment (sand, silt, or clay) are common (Figure 17a). SU4a is relatively coarser in the benchlands and finer in the plains (Figures 2 and 17b). Clasts within the diamict comprise rounded to sub-angular pebbles to boulders. Clast lithologies typically include Cordilleran quartzite, limestone and chert, locally-derived sandstone, and granite and gneiss derived from the Canadian Shield. In AWWID driller's logs, SU4a is described as clay, diamict, or till

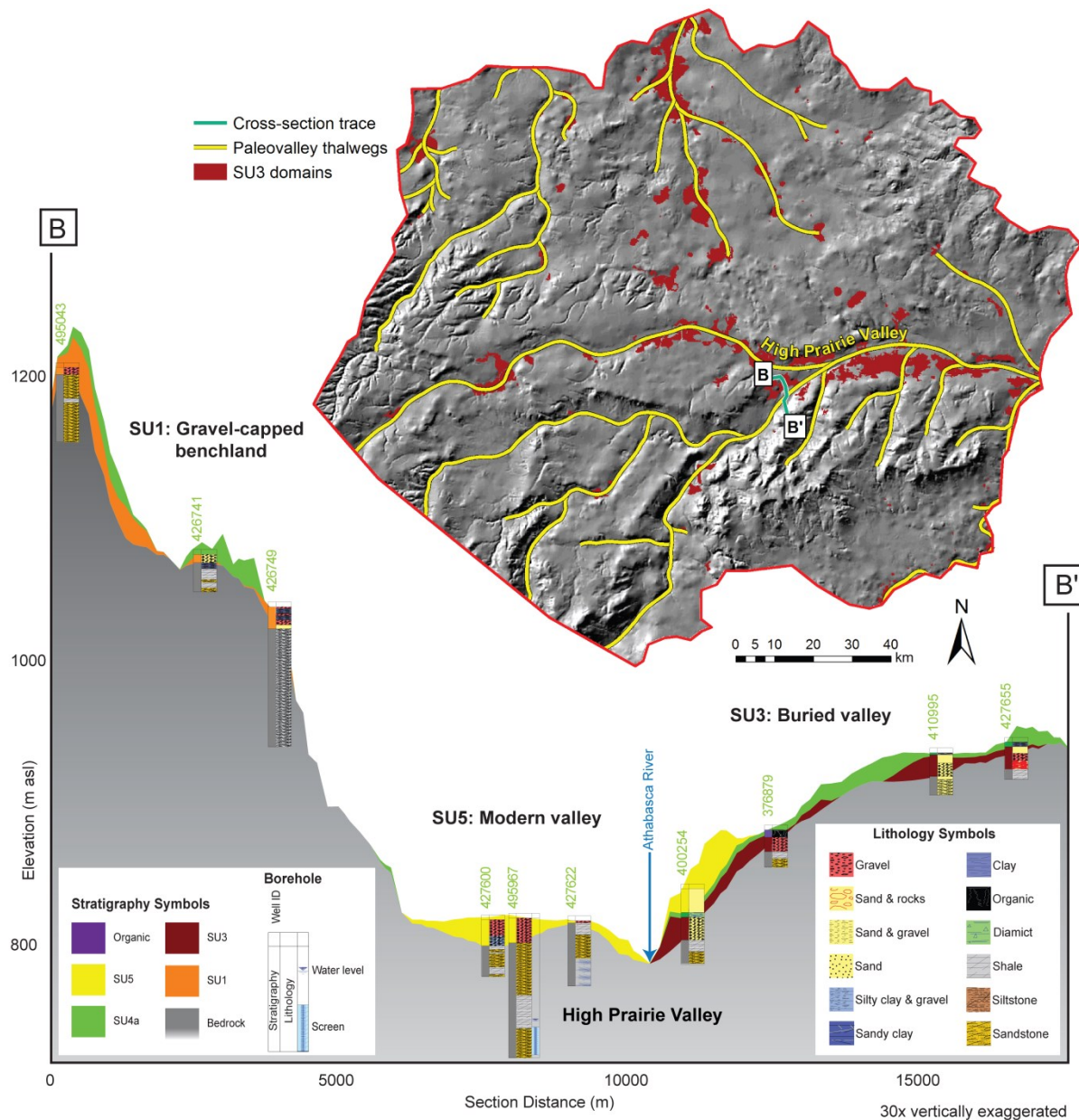


**Figure 13. Modelled extent of SU3 and location of paleovalley thalwegs overlain on a hill-shaded DEM of the bedrock topography. Cross-section B-B' shows SU3 within the High Prairie paleovalley. The unit pinches out at valley margins and is superposed by SU5.**

with several modifiers, such as boulders, coal, gravel, rocks, pebbles, sand, silt, and silty clay. Colour descriptions range from olive brown to grey or dark greyish brown (Figure 17c).

SU4a covers a large portion of WCAB (Figure 18) and comprises approximately 48% of the model volume (Table 1). The unit occurs as a relatively-uniform-thickness drape over undulating to hilly topography, averaging approximately 13 m thick (Figure 19), thickening to  $\geq 20$  m above buried valleys and within moraines (Atkinson et al., 2014) and thinning across benchlands where this unit is less continuous (cross-section B-B', Figure 13). SU4a is commonly exposed at surface, mantling bedrock and preglacial fluvial sediments (SU1 and SU3), and is in places overlain by SU4b or SU5 (Figure 9).

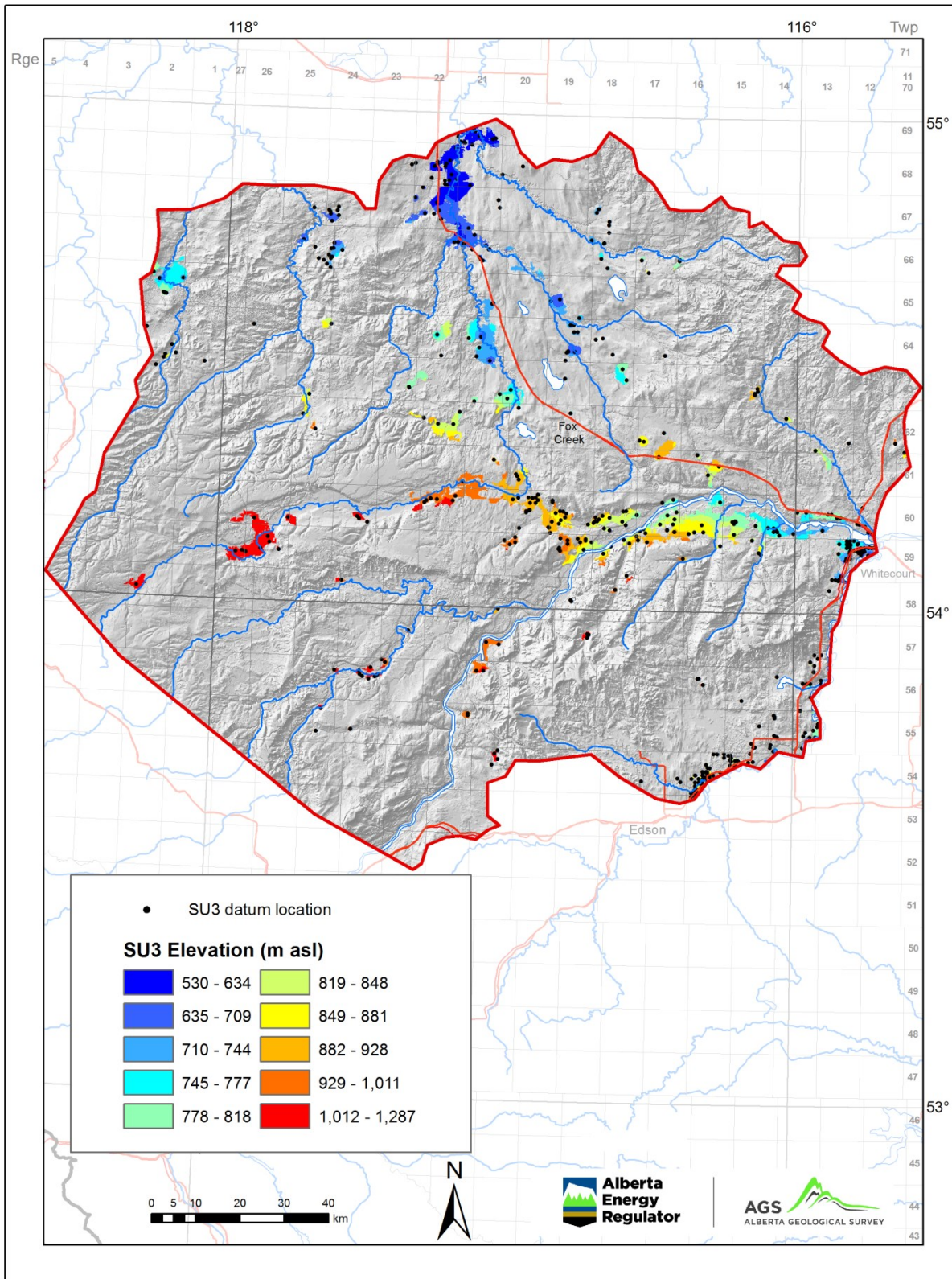


Figure 14. Hill-shaded bare-earth LiDAR DEM showing the elevation of SU3.

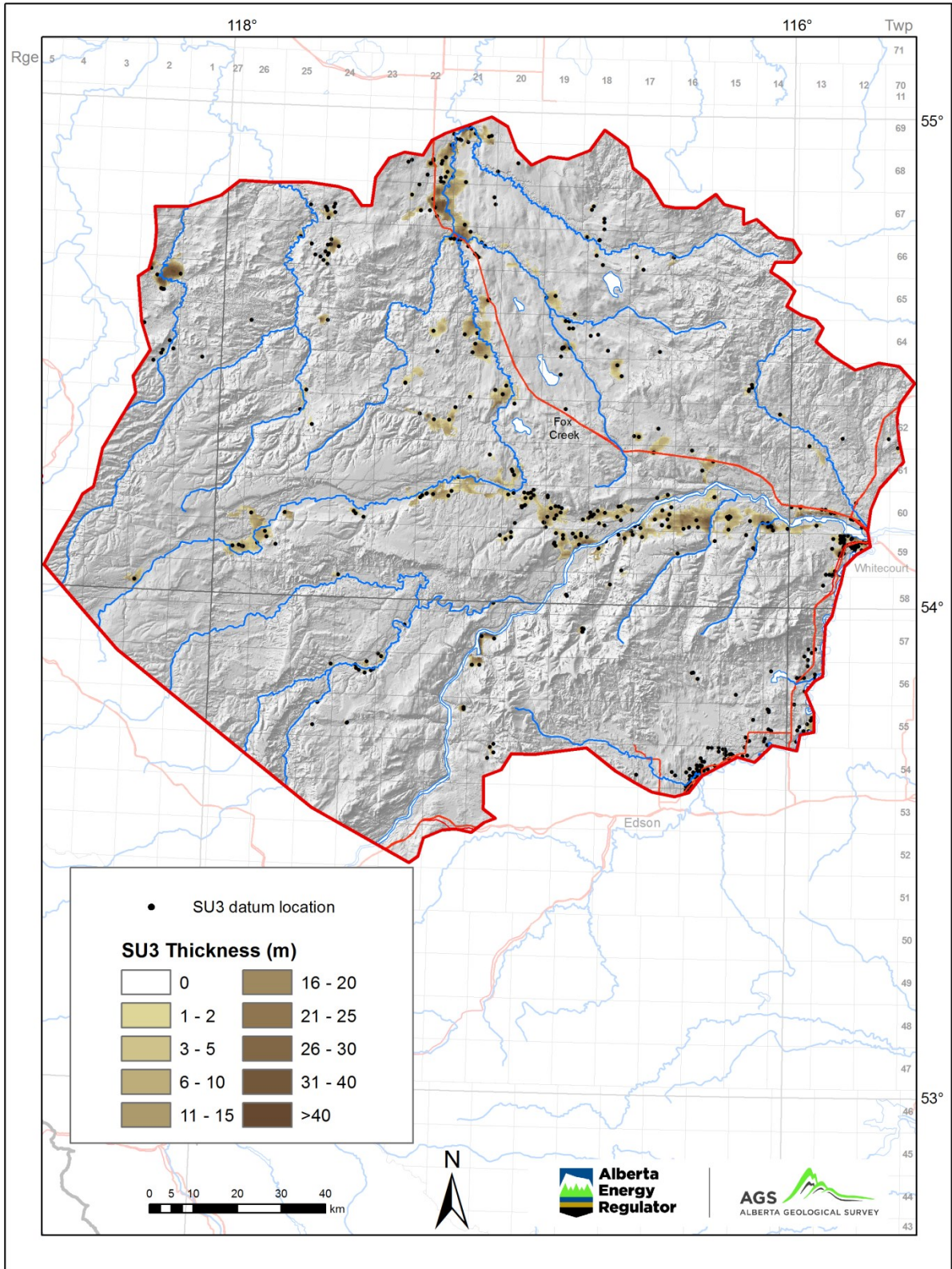
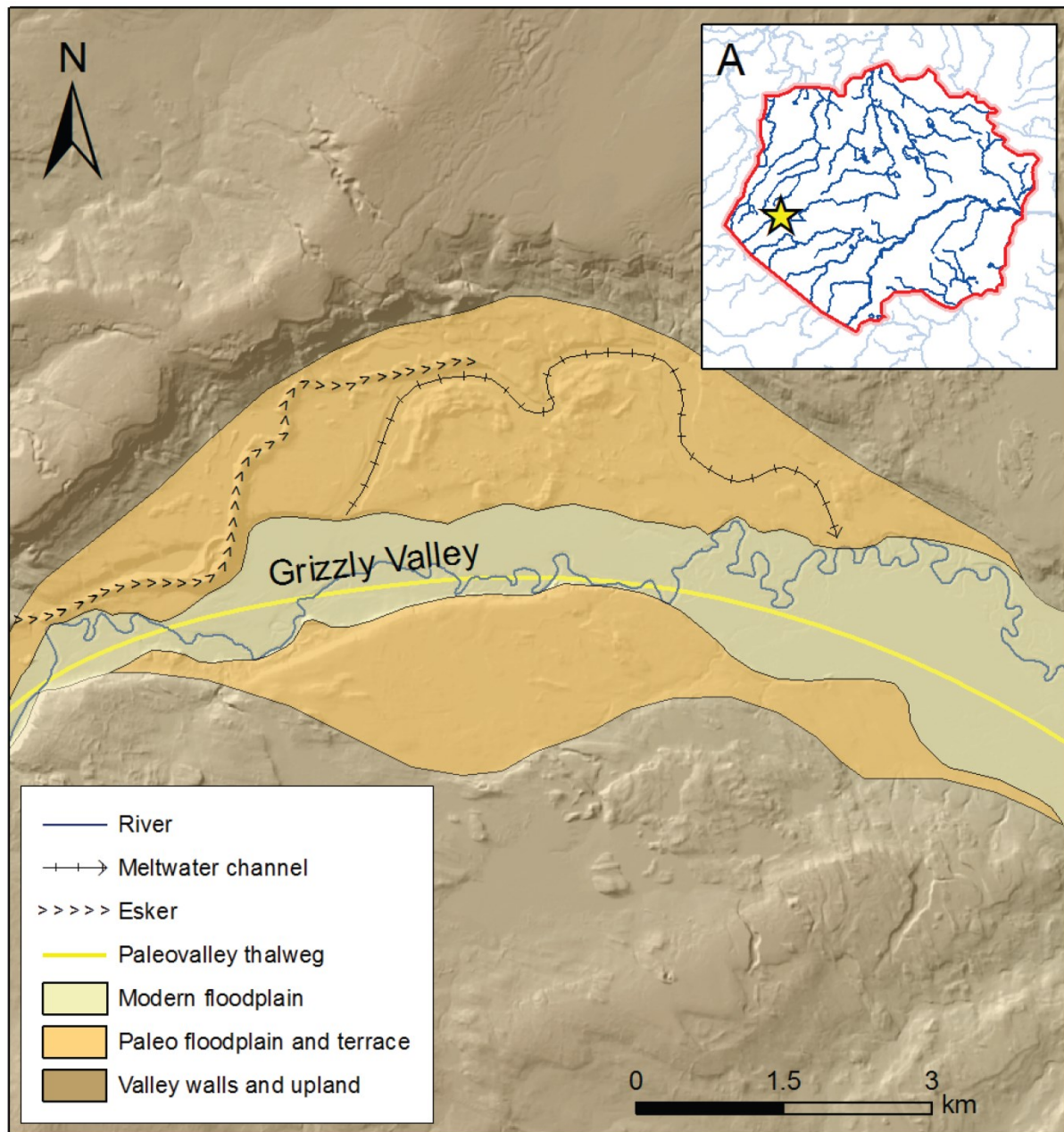


Figure 15. Hill-shaded bare-earth LiDAR DEM showing the thickness of SU3.



**Figure 16. Portions of floodplain and terraces of the preglacial Grizzly Valley (SU3) remain recognizable along this part of the Little Smoky Valley in western WCAB (inset A) even though they are superposed by an esker and meltwater channel (SU5) and scattered glacial deposits (SU4a), and are incised by the modern river (SU5).**

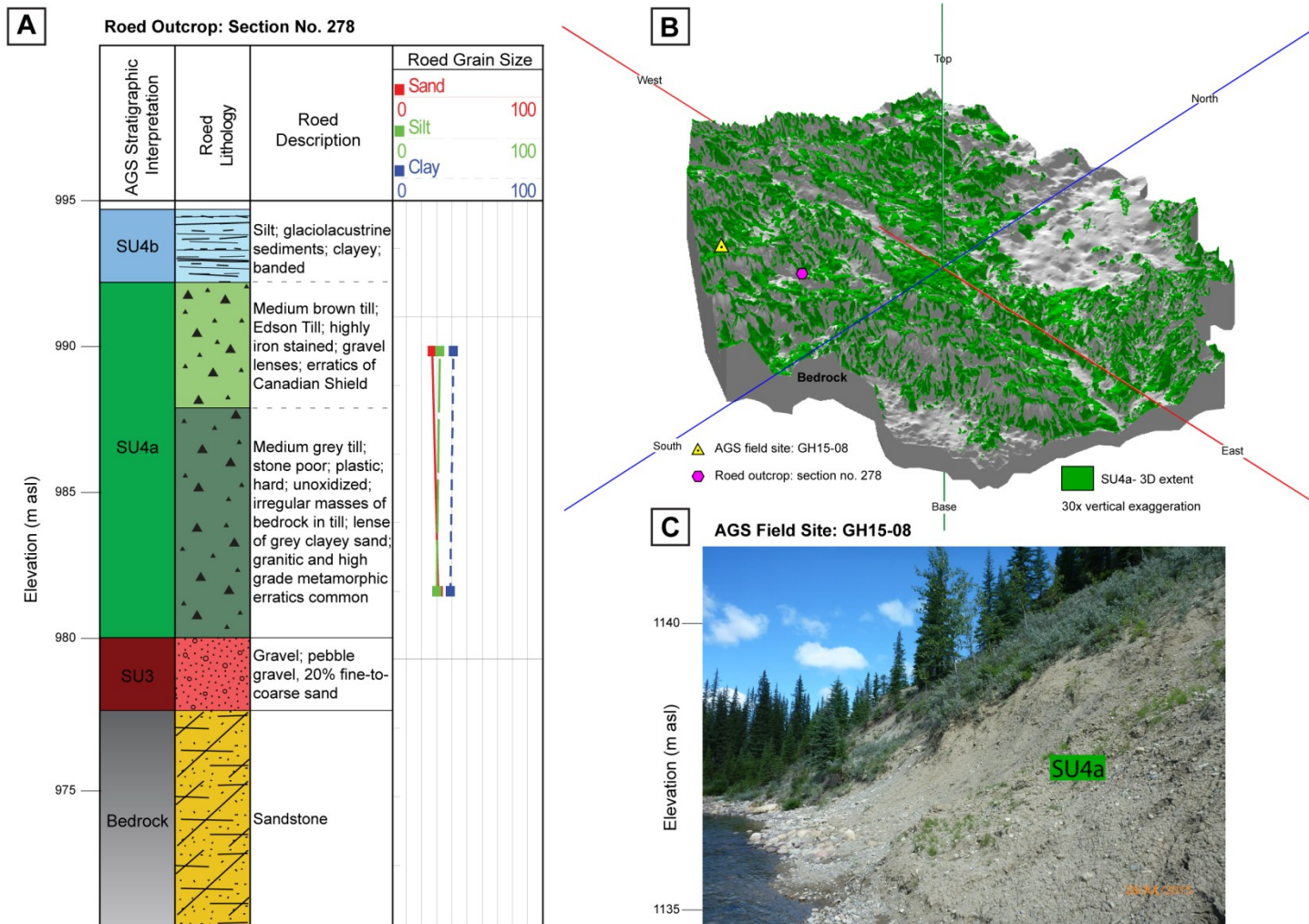


Figure 17. (a) Outcrop description (digitized from Roed, 1968) and AGS stratigraphic interpretation. (b) 3D view of SU4a overlying bedrock. (c) Photo of AGS field site showing exposure of SU4a.

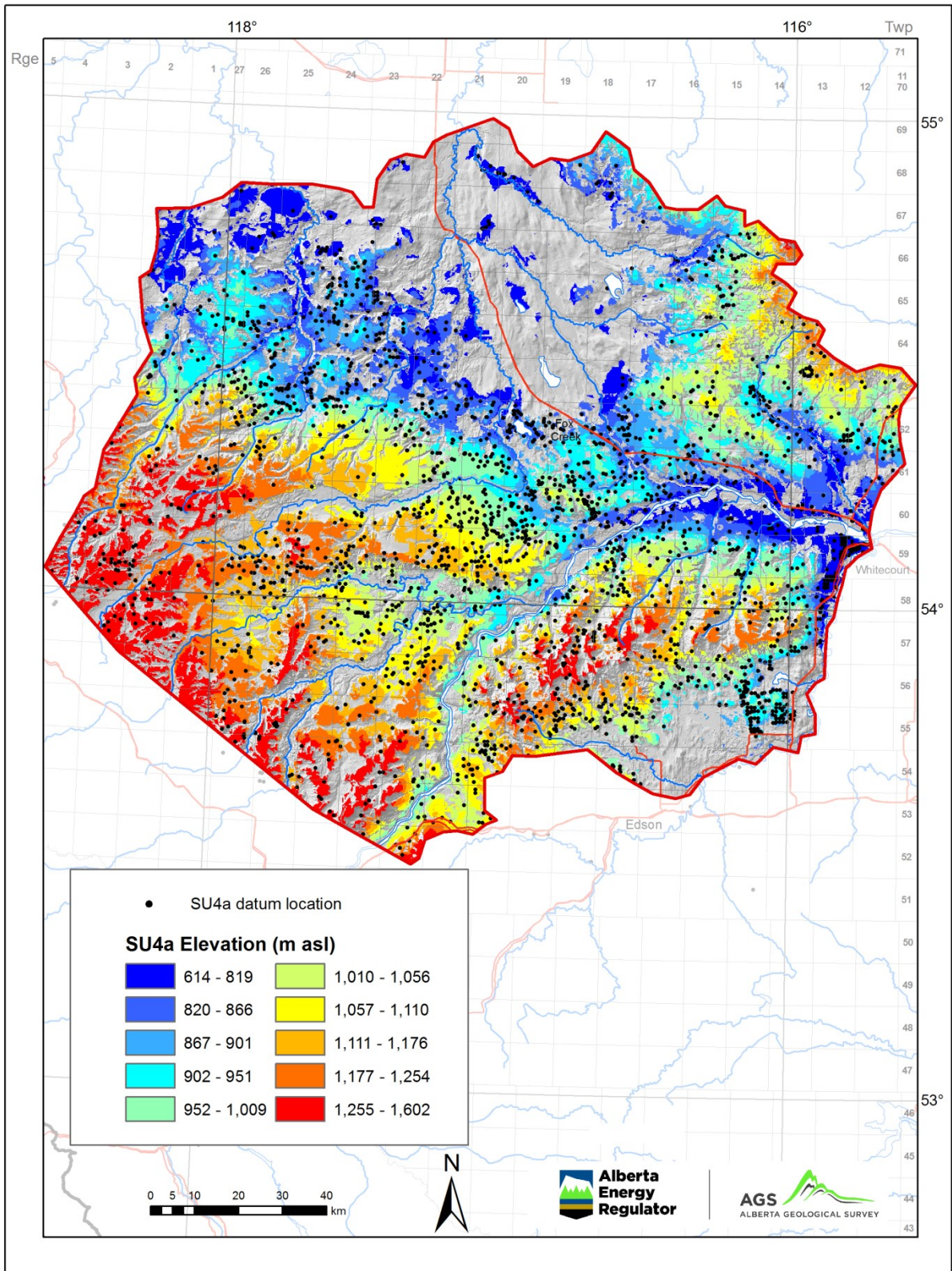


Figure 18. Hill-shaded bare-earth LiDAR DEM showing the elevation of SU4a.

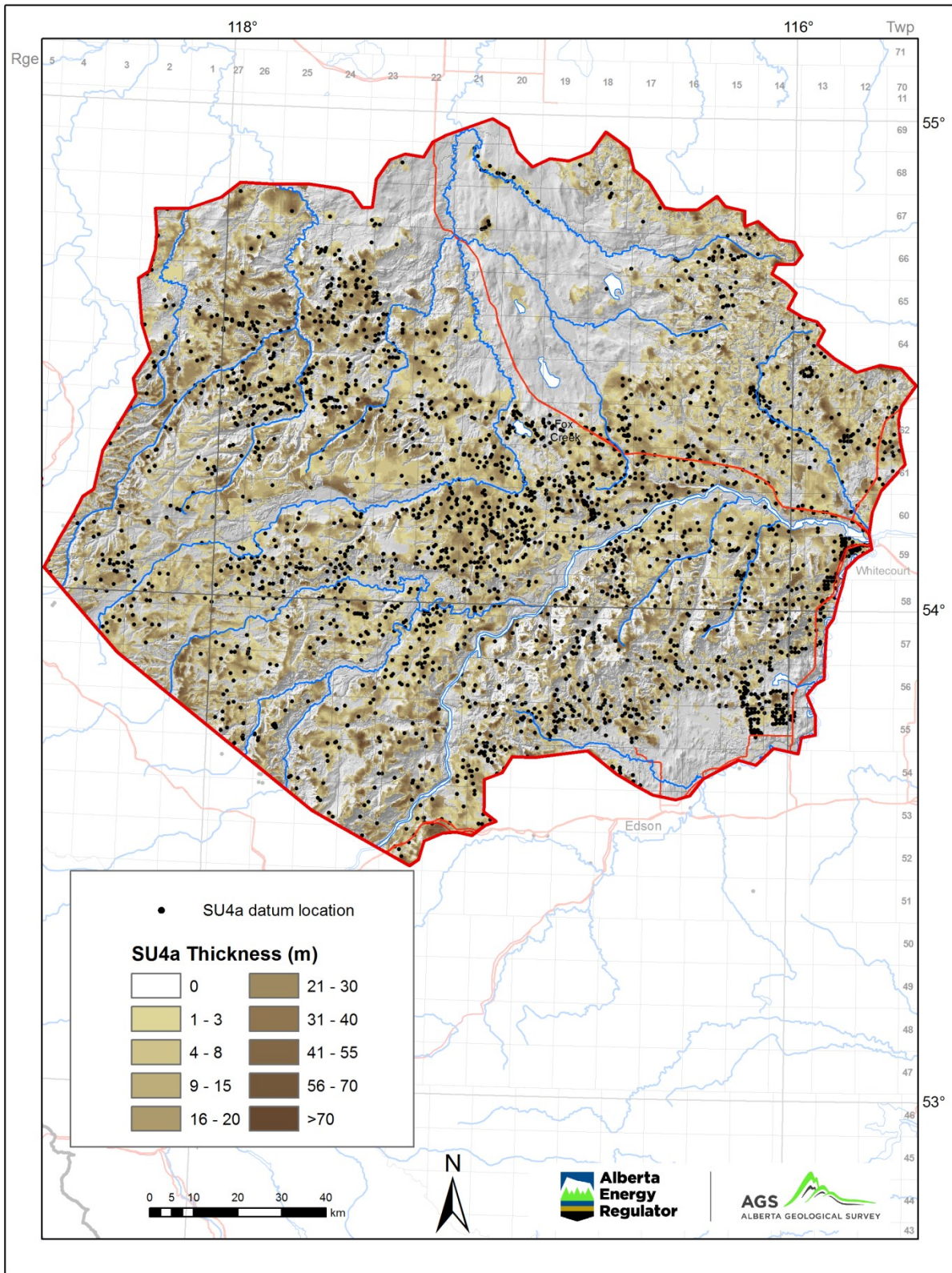


Figure 19. Hill-shaded bare-earth LiDAR DEM showing the thickness of SU4a.

Sporadically, the textural variability and topographically unconstrained distribution of SU4a made it difficult to differentiate from other stratigraphic units. The unit was mainly identified on cross-section on the basis of bulk textural properties, thickness, stratigraphic position, and landform association (Figure 5; Roed, 1968; Atkinson et al., 2016; Utting et al., 2016). In benchland settings, where SU4a is thin and relatively coarse grained, it was particularly difficult to distinguish from SU1 sand and gravel (Table 2 and Figure 10c). Consequently, it is probable that some portion of SU1 comprises Late Wisconsinan glacial diamict and that the thin and discontinuous character of SU4a is partly a function of its misidentification. Roed (1968) similarly noted difficulty in distinguishing fluvial and glacial diamicts in benchland settings.

SU4a is interpreted as a regionally extensive till sheet deposited during the Late Wisconsinan expansion of the Cordilleran and Laurentide ice sheets across WCAB (Roed, 1975; Atkinson et al., 2016). Although tills associated with these ice sheets are lithologically distinctive—containing clasts originating from Cordilleran and Laurentide source areas occurring in the southwest and northeast, respectively, and mixed lithologies occurring in the central WCAB (Roed, 1968, 1975; Atkinson et al., 2016)—the lack of petrological information in the majority of data (AWWID logs) preclude regional delineation of these diamicts, so they are included as a single unit in this study (Figure 17a and c).

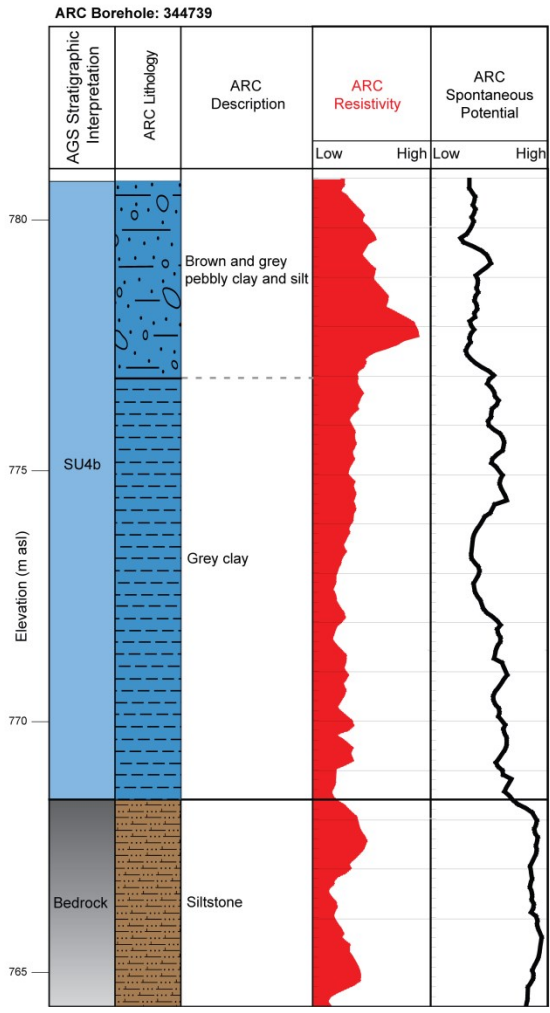
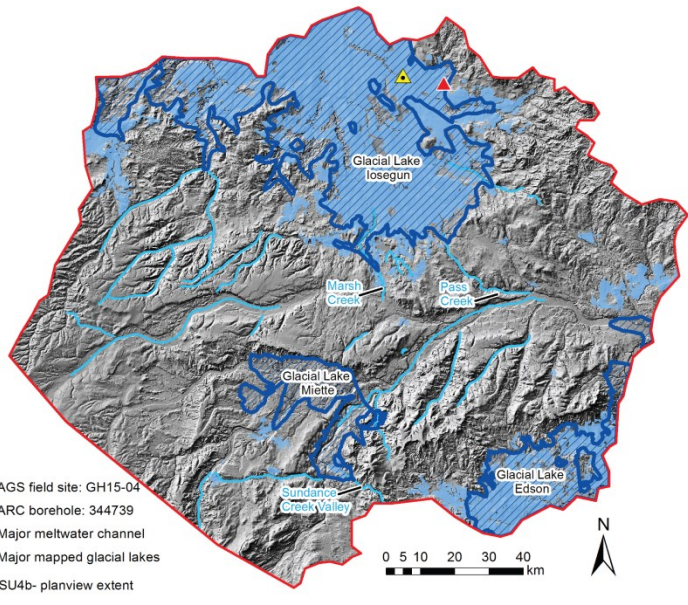
#### **6.4 SU4b: Fine-Grained Glaciolacustrine Silt, Clay, and Diamict**

SU4b includes both clay-rich diamict and massive to laminated clay and silt, undifferentiated at the scale of this study (Figure 20a). Lenses or interbeds of well-sorted sediment (sand, silt, and clay) are common within SU4b (Table 1). The unit is best described in a series of high-quality boreholes from the ARC coal survey investigations (Figure 6a) as clay and, to a lesser extent, till with varied clast content (Figure 20a). Resistivity logs from some ARC boreholes show a coarsening-upward trend within the unit (Figure 20a). Field observations along the Goose River (Figures 6b and 20b) reveal SU4b as a well-bedded clay/silt to clast-poor diamict. Lithological descriptions in the AWWID commonly include intervals consisting of sorted silt or sand. Colour descriptions from AWWID records and outcrop examinations range from blue or brown grey to dark olive grey (Figure 20c).

SU4b is confined to the north-central and southern plains in the study area (Figure 21). The unit mainly overlies bedrock and, to a lesser extent, SU4a. In some buried valleys (e.g., the Valleyview paleovalley), SU4b overlies SU3 (Balzer, 2000; Figure 13). For most of its extent, the unit is exposed at the modern land surface (Figure 9) except where it is sporadically overlain by organics and modern fluvial sediments (SU5; Figure 5). SU4b is typically 20 m thick, and is thickest and most extensive across the Iosegun and Edson plains (Figure 22).

The base of SU4b is difficult to identify, particularly where it overlies SU4a or fine-grained, poorly lithified bedrock. Within mapped glacial lake basins, undifferentiated fine-grained units were typically assigned to SU4b unless the stratigraphy in adjacent boreholes suggested otherwise. Where the unit overlies bedrock and both units were similarly described in low-quality data, high-quality ARC borehole lithologs (where available), topographic setting, and the stratigraphy of adjacent boreholes were used to guide stratigraphic interpretations. As a consequence of the difficulty in distinguishing its base, SU4b may include some unknown proportion of SU4a and bedrock.

SU4b is interpreted primarily as a glaciolacustrine deposit corresponding to the distribution of proglacial lakes across the Iosegun and Edson plains (St-Onge, 1972; Utting et al., 2015, 2016; Figures 20b, c, and 21). Diamict within the unit may record ice marginal re-advances or the influx of debris flows or ice-rafted material into lake basins. Common sand-/silt-dominated interbeds may reflect lake lowering events, sediment gravity flows, or the influence of a tributary stream on local lake basin sedimentation. The

**A****B****C**

**Figure 20. (a) Stratigraphic interpretation of ARC coal-survey borehole litholog and geophysical log. (b) Modelled extent of SU4b overlain on the hill-shaded bare-earth LiDAR DEM with the outlines of glacial lakes (modified from Utting et al., 2015, 2016). (c) Photo of AGS field site with interpreted stratigraphic unit SU4b.**

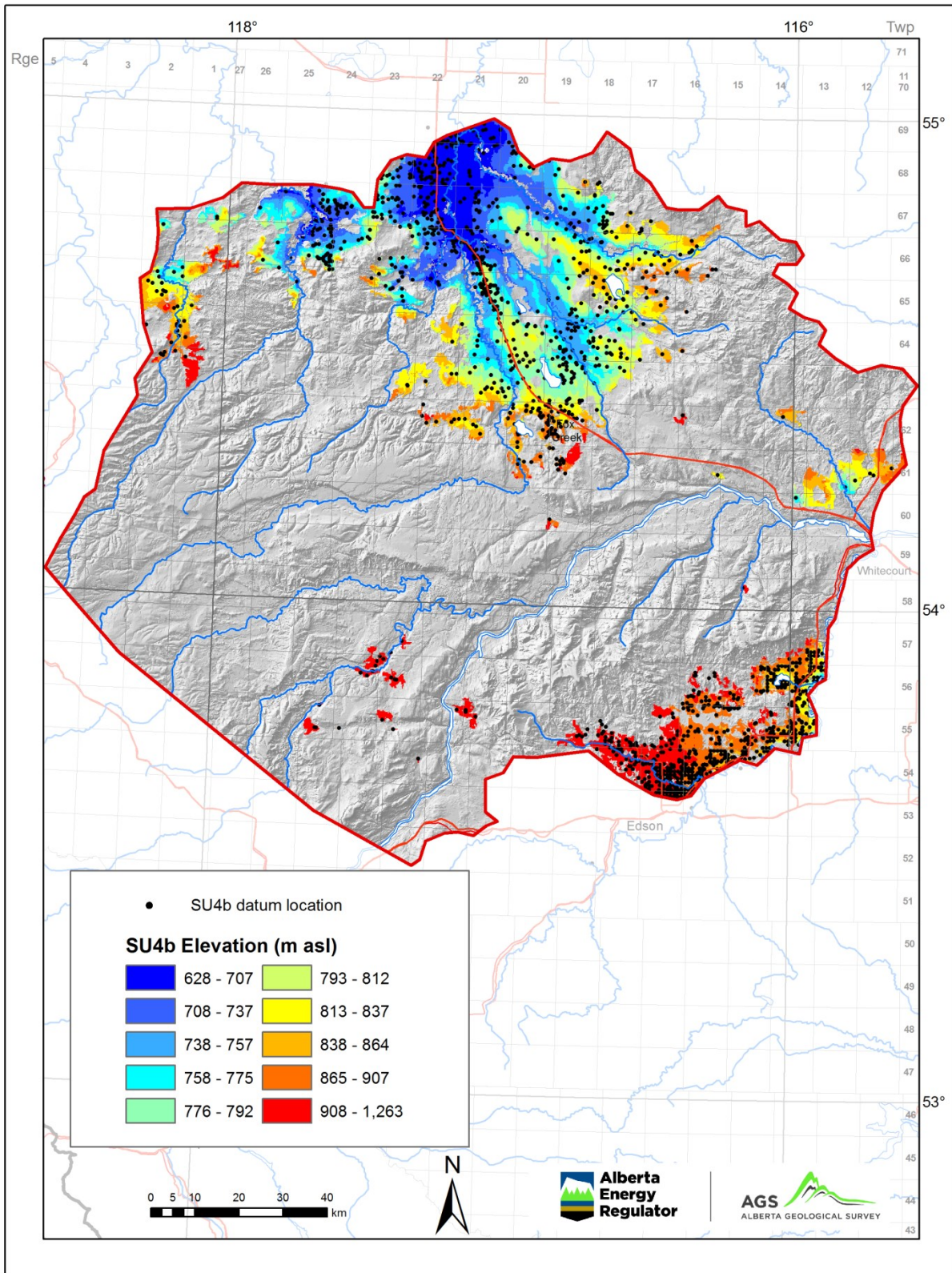


Figure 21. Hill-shaded bare-earth LiDAR DEM showing the elevation of SU4b.

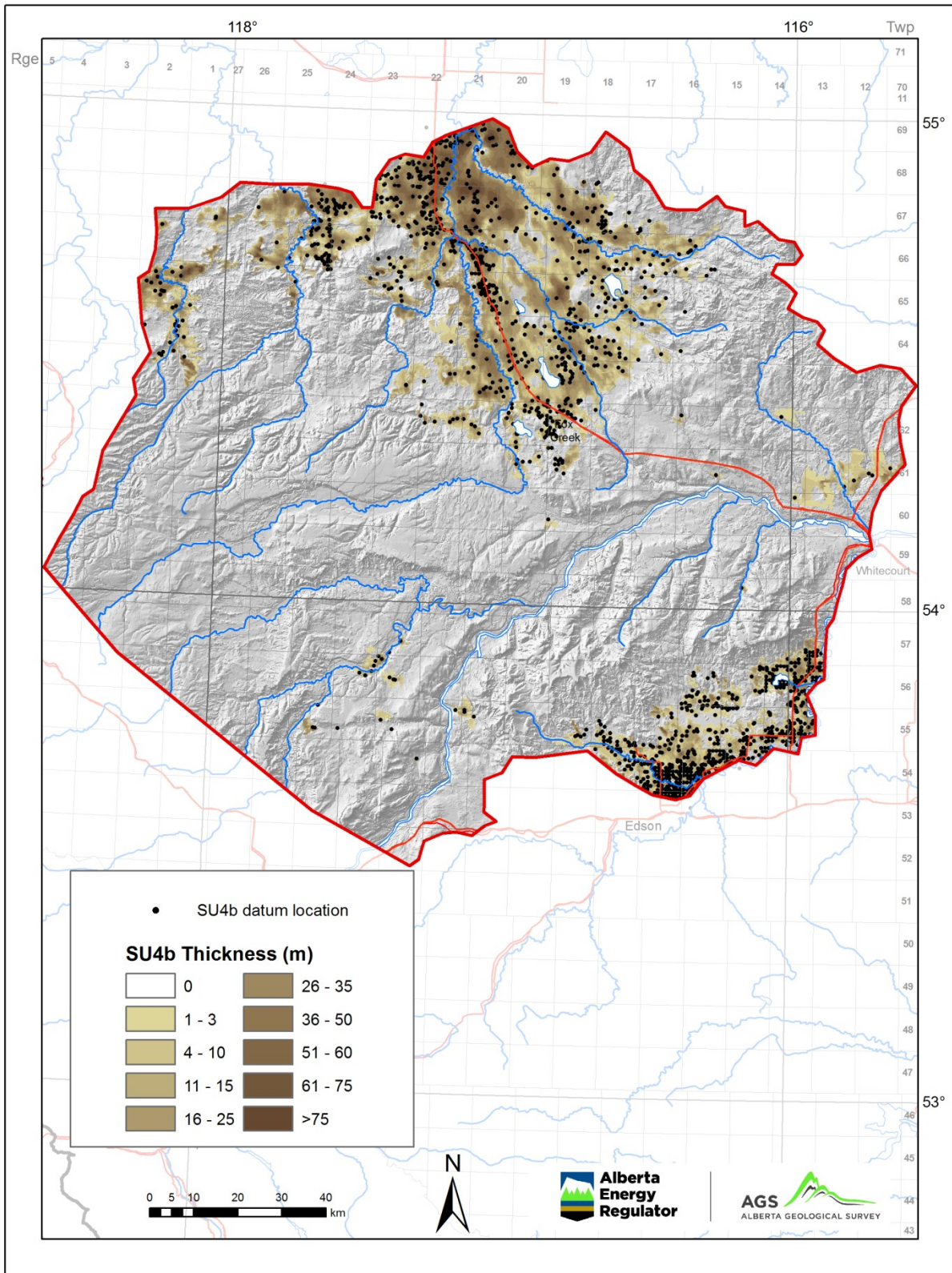


Figure 22. Hill-shaded bare-earth LiDAR DEM showing the thickness of SU4b.

thickest accumulations are consistent with central positions of the lake basins as well as superposition above buried valleys (Figure 22).

## **6.5 SU5: Fluvial and Glaciofluvial Sand and Gravel and Eolian Sand**

SU5 comprises a surficial assemblage of well-sorted, massive to horizontally bedded to ripple cross-bedded silt, sand, and rounded to sub-round boulder gravel (Figure 23a; cross-section C-C', Figure 23). Clast lithologies include quartzite, chert, limestone, conglomerate, sandstone, and, in the central and eastern parts of WCAB, pink granitoid gneiss derived from the Canadian Shield (Figure 4; Roed, 1968, 1975; Atkinson et al., 2016). SU5 in AWWID logs and AGS field sites is light brown to grey, olive brown, tan or yellow (Figure 23c).

SU5 is found within all physiographic regions (Figures 2 and 24), where it is closely associated with fluvial, glaciofluvial, and eolian landforms (Figure 23a) and, to a lesser extent, modern and paleolakes. Consequently, SU5 occurs within channels and floodplains, eskers, shorelines, and dune fields (Figure 5). With the exception of dune fields, these landforms, and consequently the geometry of SU5, are typically linear. In dune fields, however, SU5 may form a broad to locally discontinuous blanket. Unit thickness is highly varied as the relatively narrow fluvial and glaciofluvial deposits pinch out abruptly at valley or channel margins (cross-section C-C', Figure 23). Relatively thick deposits (Figure 25) occur along the axis of modern river valleys, including the Athabasca, Wildhay, and Berland rivers, and to a lesser extent the Little Smoky River. The thickest, most extensive deposits occur where dune fields superpose glaciofluvial outwash and fluvial plains (e.g., the Windfall Plain and at the confluence of the Wildhay and Berland Rivers). SU5 may overlie all other stratigraphic units (SU1–SU4b) and is buried only by minor occurrences of organic deposits (Figure 5). The base of the unit is commonly defined by an erosional unconformity.

SU5 can be easily differentiated where it overlies fine-grained sediments such as bedrock or diamict (SU4a and SU4b), although identification becomes more challenging when underlying units are similarly coarse-grained (SU1 or SU3). This is especially the case where those units are exposed at surface or are shallowly buried, such as in the upper southwestern reaches of major river valleys and across the benchlands (Figure 16). In these areas, unit delineation was informed by surficial maps (Figures 5 and 23a). However, due to the resolution of the model, it is assumed that some undetermined portion of the SU5 model volume may include components of SU1 and SU3.

SU5 is interpreted as stratified fluvial, glaciofluvial, eolian, and littoral sediments, incorporating active and inactive deposits spanning the onset of regional deglaciation to modern time. The amalgamation of deposits with such varied genesis and depositional history reflects the similar sedimentological description (commonly sand, sand and gravel, or similar in AWWID records), stratigraphic position of these deposits (exposed at surface), their limited lateral distribution, and the scale and purpose of the model.

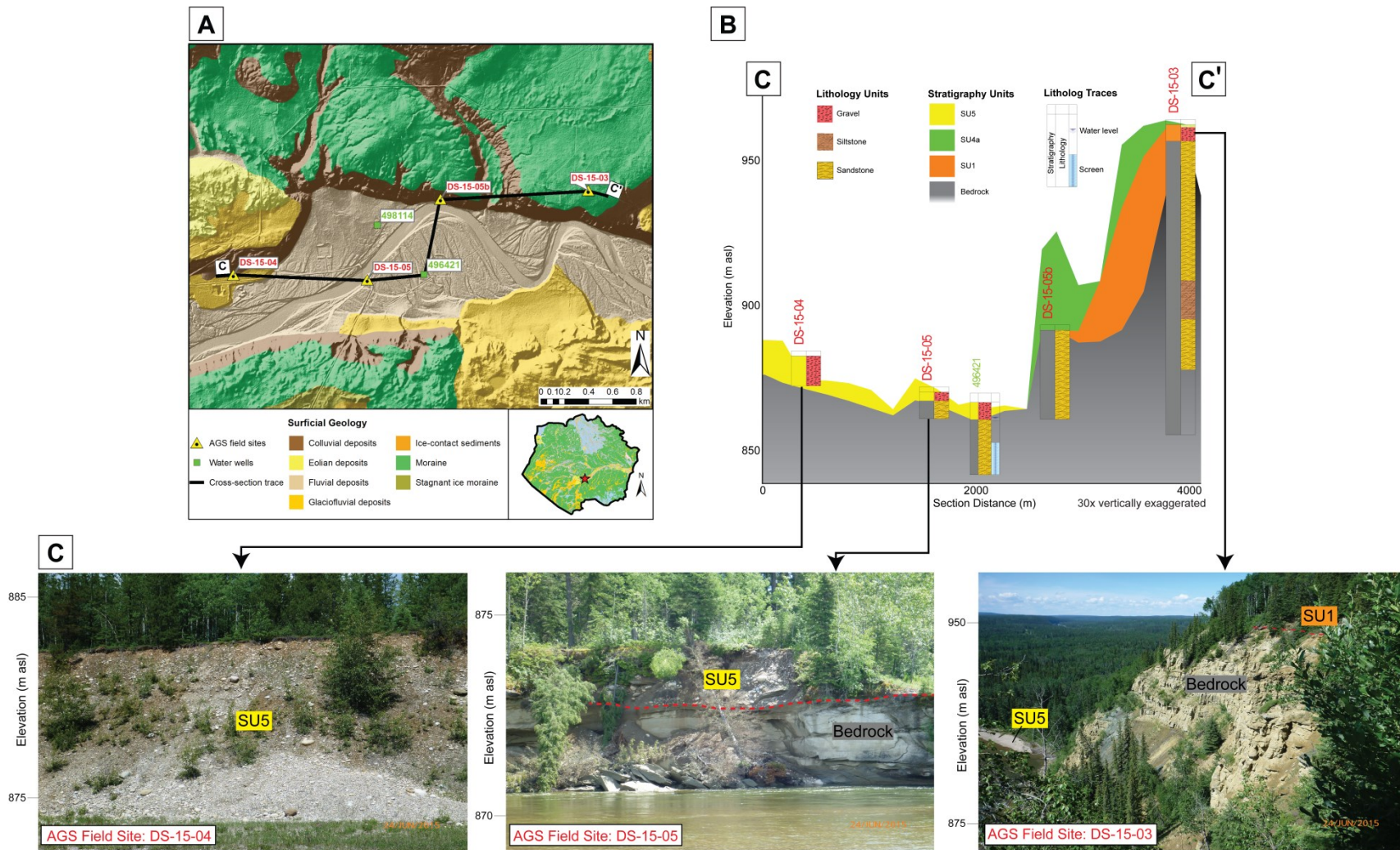


Figure 23. (a) Surficial map (from Utting, 2013) showing the distribution of eolian, fluvial, and glaciofluvial sediments, classed as SU5, and the location of cross-section C-C'. (b) Cross-section C-C' of the model shows SU5 infill of a valley incised into bedrock along the present-day Berland River. (c) Photos of AGS field sites showing exposure of sediments classed as SU5. Photos correspond to litholog traces on cross-section C-C'.

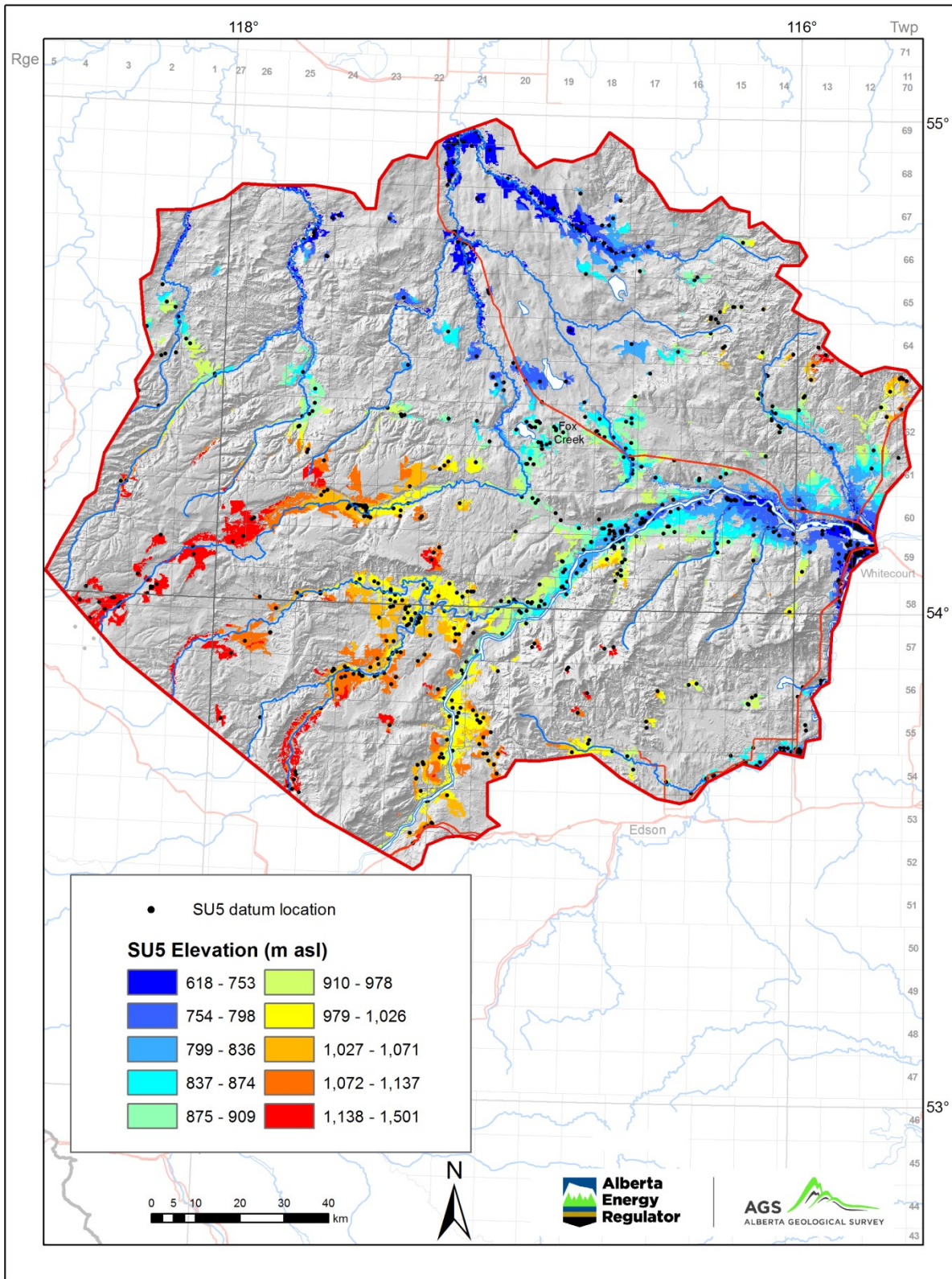


Figure 24. Hill-shaded bare-earth LiDAR DEM showing the elevation of SU5.

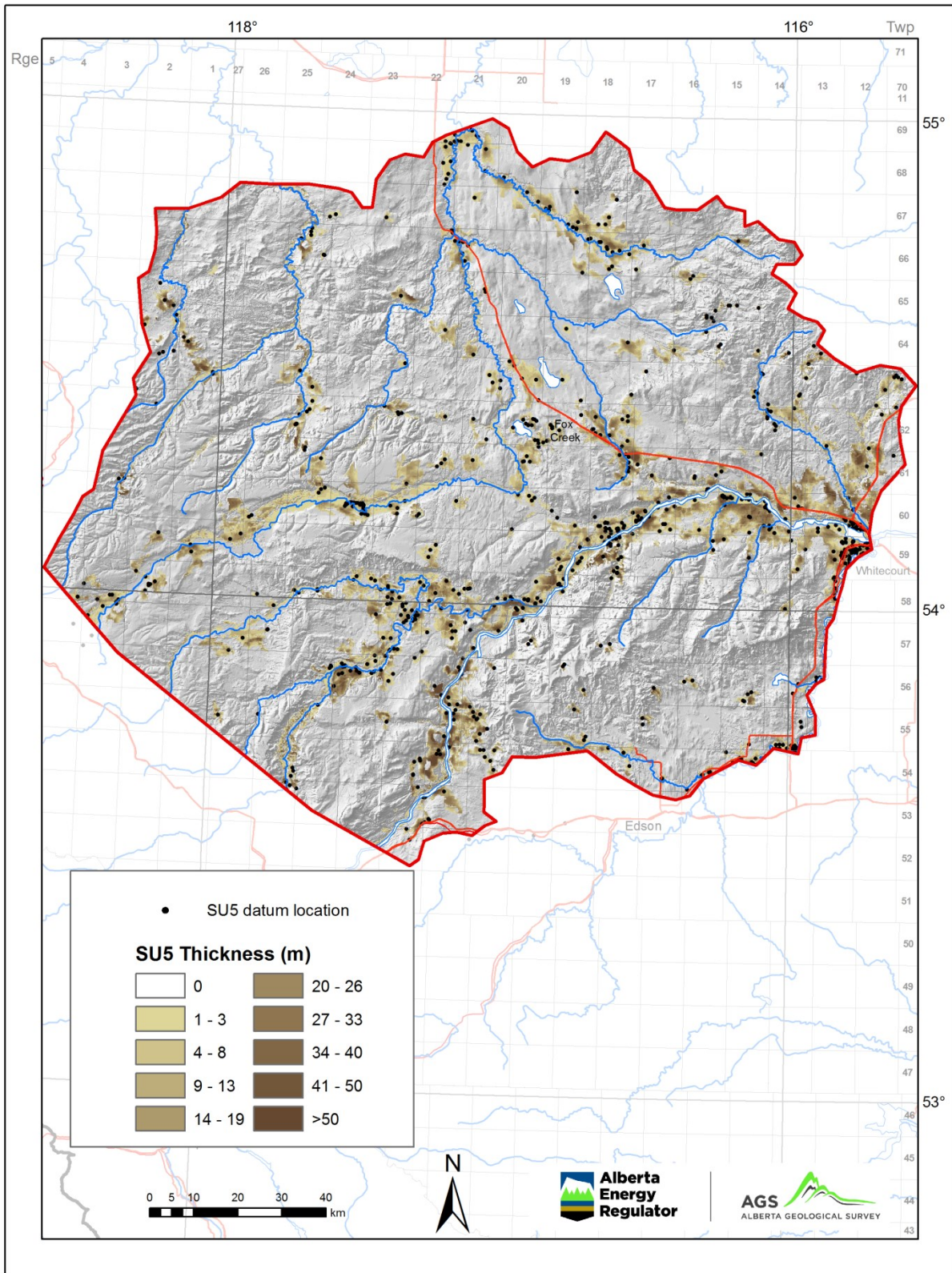


Figure 25. Hill-shaded bare-earth LiDAR DEM showing the thickness of SU5.

## 7 Model Limitations and Uncertainty

These mappable stratigraphic units form the components of a 3D geological model of the Paleogene–Quaternary succession based on the authors’ conceptual understanding of the subsurface. This model provides a regional-scale framework and characterization of the subsurface within the limits of available data. As the subsurface is not uniformly sampled, model uncertainty needs to be accounted for, including the diverse and complex nature of input datasets (Figure 6), interpretation error due to geological complexity, non-uniform distribution and density of subsurface information, and model construction that extrapolates gridded-surface information from known data points (Figure 26).

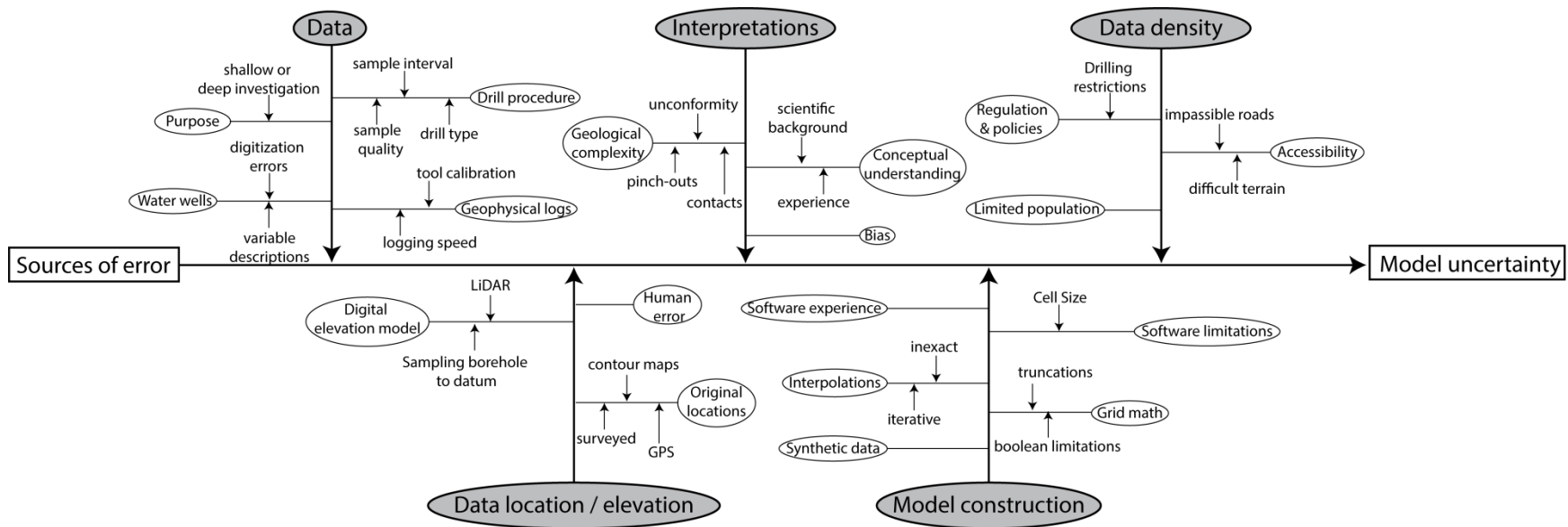
Input datasets for the model were derived from multiple sources of varying location and description quality and compiled in the lithological database. Data with accurate geospatial locations and lithological descriptions made by a geoscientist were deemed to be of high-to very-high quality and account for approximately 20% of subsurface data used in this study (Figure 27). The use of lower-quality data is assessed against these higher-quality datasets, as is the case of AWWID records, which are calibrated to AGS field observations. About 20% of the calibrated water-well information was found to be located within 1 km of a high-quality point. However, this calibration procedure was not possible in parts of WCAB where data were sparse (dark blue patterns, Figure 27). The authors recognize regions in the model that have greater uncertainty due to sparse data, especially where ground access is difficult (Figure 6b). In areas of highly varied geology, any drastic changes in lithology between subsurface data points would require a higher density of data to accurately represent the geometry of stratigraphic units. Model construction also introduces errors in rendering the geometry of stratigraphic units due to either the interpolation procedure selected or subsequent grid-math modifications.

Table 3 outlines the root mean square error (RMSE) for each modelled grid. This is a summary statistic that globally quantifies how far input points used for the interpolation of a grid for each stratigraphic unit deviate vertically from the grid (MacCormack et al., 2013). Gridded-surfaces were rendered iteratively to allow for the analysis of outliers and to ensure that the RMSE was as low as possible.

The 3D geological model developed for this study is appropriate only for regional-scale use (1:100 000). This model is not intended to be used in place of site-specific investigations because its accuracy is constrained by the data quality, quantity, distribution, and geological complexity at that scale (200 m grid cell size). This model is reproducible because the source stratigraphic interpretations are managed in a database that can be easily modified to enable new renderings. With new data and stratigraphic interpretations, revisions of this model can be linked with other models created elsewhere in the province to fit into a new hydrostratigraphic framework.

## 8 Development of a Hydrostratigraphic Model of the Paleogene–Quaternary Deposits

The attribution of hydraulic information to the stratigraphic interpretations enables hydrostratigraphic units to be derived from stratigraphic units (Maxey, 1964; Seaber, 1988). Mapping hydraulic properties within the Paleogene–Quaternary succession has the potential to inform additional subdivisions or combinations of stratigraphic units due to either similarities or contrasts in hydraulic properties. This may be the case for coarse-grained deposits that have a high degree of hydraulic connectivity and are mappable at the regional scale (1:100 000). Coarse-grained sediments (SU1, SU3, and SU5) account for approximately 25% of the model volume (Table 1) and could potentially form local-scale aquifers within WCAB. The degree of hydraulic connectivity within individual units and potentially between different coarse-grained units would have to be established through mapping of hydraulic head conditions or using



**Figure 26. Sources of error contributing to model uncertainty (Lelliott et al., 2009). Shaded ovals represent the major sources of error, which are divided into smaller subsets to illustrate the numerous factors that can contribute to overall uncertainty. The most prominent sources of error include the input data and interpretation of lithological descriptions as distinct stratigraphic units.**

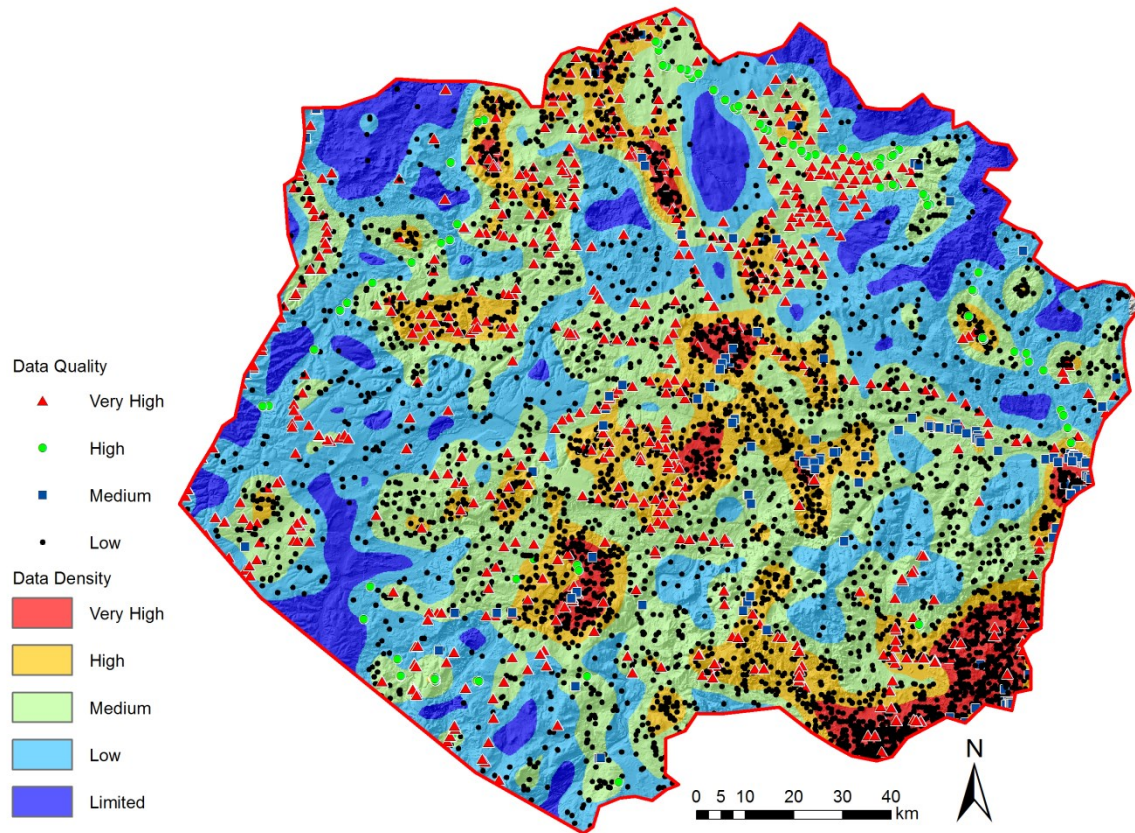


**Figure 27. Density of input data. Overlying data points are classed according to the quality defined in Figure 6. There is a divergence in many cases between data quality and density, where sparse areas may have high-quality data and dense areas may have lower-quality data.**

**Table 3. RMSE values for gridded surfaces used to construct 3D model.**

| Stratigraphic Unit (SU) | Number of Stratigraphic Assignments | RMSE (m) |
|-------------------------|-------------------------------------|----------|
| SU5                     | 734                                 | n/a      |
| SU4b                    | 1647                                | 3.15     |
| SU4a                    | 2303                                | 5.07     |
| SU3                     | 418                                 | 2.06     |
| SU1 / SU2               | 844                                 | 3.15     |
| Bedrock topography      | 17997                               | 3.46     |

\* RMSE for SU5 is not reported because the top of SU5 was made equal to the modern land surface topography.

a groundwater flow model. The remaining stratigraphic units are considered fine-grained and account for approximately 75% of the modelled volume (Table 1). SU4a is the most extensive fine-grained unit in the model and could have a lower potential as a groundwater resource, though locally coarse-grained deposits

are included. Hydraulic information could provide insights into the effectiveness of these fine-grained stratigraphic units as confining layers.

Ultimately, the underlying bedrock units are the preferred units for groundwater withdrawals for industry because they are the most significant hydrogeological features in the study area and comprise WCAB's major groundwater resources (Grasby et al., 2008; Hughes et al., 2017). Closer examination of the hydrostratigraphic units and hydraulic head conditions would help better understand the relationship between the shallow Paleogene–Quaternary sediments and bedrock strata. Considering the physical properties of the stratigraphic units described in the 3D geological model presented in this report, it can be assumed that the thickness and distribution of coarse-grained and fine-grained sediments will strongly influence groundwater recharge. Where surficial sediments are able to transmit water easily, recharge to underlying bedrock strata will be enhanced. In addition, areas of bedrock that are underlain by sand-rich diamicts of SU4a or sand and gravel of SU1 or SU3, and which are close to the land surface, may be more susceptible to the migration of surface contaminants.

## 9 Conclusions

The shallow 3D geological model presented in this report provides a regional-scale (1:100 000) rendering of Paleogene–Quaternary stratigraphic units in west-central Alberta. The model is based upon lithological data sourced from AWWID water-well records, AGS drillholes, ARC coal surveys, AEP information, industry mineral core, field logs, and GIS layers of spatial datasets. However, the identification and correlation of mappable stratigraphic units was fundamentally guided by a conceptual stratigraphy of the study area in which the genesis and predicted spatial distribution of stratigraphic units was rationalized. Stratigraphic units were defined on cross-sections using high-quality data collected from field investigations, which were then used to calibrate variable-to-low-quality data, to create mappable units at a regional scale. The stratigraphic units mapped in this study include gravel caps on bedrock benchlands largely emplaced by preglacial fluvial planation and deposition (SU1); sporadically distributed gravel on plains (SU2) and grouped with SU1; buried-valley gravel emplaced within preglacial valleys and glacial meltwater channels (SU3); coarse-grained glaciogenic diamict comprising mainly till (SU4a); fine-grained glaciogenic diamict largely comprising glaciolacustrine sediment (SU4b); and fluvial or glaciofluvial sand and gravel, and eolian sand exposed at surface along modern valleys, glaciofluvial drainage-paths, and dune fields (SU5). Subdivision of the Paleogene–Quaternary succession into these stratigraphic units facilitates a general categorization of shallow subsurface sediments as approximately 25% coarse-grained and 75% fine-grained materials. Rendering these Paleogene–Quaternary stratigraphic units in 3D contributes to the integrated assessment of the geology and hydrogeology of WCAB and provides information needed to support land-use planning and resource management decisions in the shallow subsurface.

## 10 References

- Alberta Environment and Parks (2006): Water conservation and allocation policy for oilfield injection; Alberta Water for Life Pub No. 1/969, URL <<http://aep.alberta.ca/water/programs-and-services/groundwater/regulation-and-policy/documents/WaterConservationOilfieldInjectionPolicy.pdf>> [September 2016].
- Alberta Environment and Parks (AEP) (2015): Alberta water well information database (Microsoft Access format, downloaded May 2015); Alberta Environment and Parks, URL <<http://aep.alberta.ca/water/reports-data/alberta-water-well-information-database/default.aspx>> [May 2015].
- Alden, W.C. (1932): Physiography and glacial geology of eastern Montana and adjacent areas; U.S. Geological Survey, Professional Paper 174, 133 p.
- Atkinson, N. and Pawley, S.M. (2013): Surficial geology of the Crooked Lake area (NTS 83K/SW); Energy Resources Conservation Board, ERCB/AGS Map 563, scale 1:100 000, URL <[http://ags.aer.ca/publications/MAP\\_563.html](http://ags.aer.ca/publications/MAP_563.html)> [June 2015].
- Atkinson, N., Utting, D.J. and Pawley, S.M. (2014): Landform signature of the Laurentide and Cordilleran ice sheets across Alberta during the last glaciation; Canadian Journal of Earth Sciences, NRC Research Press, v. 51, no. 12, p. 1067–1083.
- Atkinson, N., Pawley, S. and Utting, D.J. (2016): Flow-pattern evolution of the Laurentide and Cordilleran ice sheets across west-central Alberta, Canada: implications for ice sheet growth, retreat and dynamics during the last glacial cycle; Journal of Quaternary Science, v. 31, p.753–768.
- Atkinson, N., Utting, D.J. and Pawley, S.M. (2017): Surficial geology of west-central Alberta (NTS 83E, 83F, 83G, 83J, 83K, 83L); Alberta Energy Regulator, AER/AGS Map 582, scale 1:250 000.
- Andriashek, L.D. (2001): Surficial Geology of the Wapiti Area (NTS 83L); Alberta Energy and Utilities Board, EUB/AGS Map 239, scale 1:250,000, URL <[http://ags.aer.ca/publications/MAP\\_239.html](http://ags.aer.ca/publications/MAP_239.html)> [February 2017].
- Balzer, S.A. (2000): Quaternary geology and dispersal patterns Winagami region, Alberta; Alberta Energy and Utilities Board, EUB/AGS Special Report 14, 355 p., URL <[http://ags.aer.ca/publications/SPE\\_014.html](http://ags.aer.ca/publications/SPE_014.html)> [September 2016].
- Bostock, H.S. (1970): Physiographic Regions of Canada; Geological Survey of Canada, Map 1254A, scale 1:5 000 000.
- Bruce, J.P., Cunningham, W., Freeze, A., Gillham, R.C.M., Gordon, S., Holysh, S., Hruday, S., Logan, W., MacQuarrie, K., Muldoon, P., Nowlan, L., Pomeroy, J., Renzetti, S., Sherwood Lollar, B. and Therrien, R. (2009): The sustainable management of groundwater in Canada: the expert panel on groundwater; Council of Canadian Academies, Ottawa, Canada, 254 p., URL <<http://www.scienceadvice.ca/en/assessments/completed/groundwater.aspx>> [February 2017].
- Carlson, V.A. and Green, R. (1979): Bedrock topography of the Iosegun lake map area NTS 83K, Alberta; Alberta Research Council, Map 065, scale 1:250 000, URL <[http://ags.aer.ca/publications/MAP\\_065.html](http://ags.aer.ca/publications/MAP_065.html)> [June 2015].
- Catto, N., Liverman, D.G.E., Bobrowsky, P.T. and Rutter, N. (1996): Laurentide, cordilleran, and montane glaciation in the western Peace River–Grande Prairie region, Alberta and British Columbia, Canada; Quaternary International, v. 32, p. 21–32.
- Chu, M. (1978): Geology and coal resources of the Wapiti Formation of north central Alberta; Alberta Research Council, Open File Report 1978-12, 25 p., URL <[http://www.ags.aer.ca/publications/OFR\\_1978\\_12.html](http://www.ags.aer.ca/publications/OFR_1978_12.html)> [October 2016].

- Dawson, F.M., Kalkreuth, W.D. and Sweet, A.R. (1994a): Stratigraphy and coal resource potential of the Upper Cretaceous to Tertiary strata of northwestern Alberta; Geological Survey of Canada, Bulletin 466, 64 p.
- Dawson, F.M., Evans, C.G., Marsh, R. and Richardson, R. (1994b): Uppermost Cretaceous and Tertiary strata of the Western Canada Sedimentary Basin; *in* Geological Atlas of the Western Canada Sedimentary Basin, G.D. Mossop and I. Shetsen. (comp.), Canadian Society of Petroleum Geologists and Alberta Research Council, p. 387–406, URL <<http://ags.aer.ca/publications/chapter-24-uppermost-cretaceous-and-tertiary-strata>> [May 2016].
- Demchuk, T.D. and Hills, L. (1991): A re-examination of the Paskapoo Formation in the central Alberta Plains: the designation of three new members; Canadian Society of Petroleum Geologists Bulletin, v. 39, no. 3, p. 270–282.
- Dyke, A.S., Andrews, J.T., Clark, P.U., England, J.H., Miller, G.H., Shaw, J. and Veillette, J.J. (2002): The Laurentide and Innuitian ice sheets during the Last Glacial Maximum; Quaternary Science Reviews, v. 21, p. 9-31.
- Edwards, D.W.A. and Scafe, D. (1996): Mapping and resource evaluation of the Tertiary and preglacial sand and gravel formations of Alberta; Alberta Energy, Alberta Geological Survey Open File Report 1994-06, 246 p., URL <[http://ags.aer.ca/publications/OFR\\_1994\\_06.html](http://ags.aer.ca/publications/OFR_1994_06.html)> [June 2016].
- Edwards, W.A.D., Budney, H.D., Berezniuk, T. and Cadrin, M.J. (2006): Sand and gravel deposits with aggregate potential Iosegun Lake, Alberta (NTS 83K); Alberta Energy and Utilities Board, , EUB/AGS Map 299, scale 1:250 000, URL <[http://ags.aer.ca/publications/MAP\\_299.html](http://ags.aer.ca/publications/MAP_299.html)> [June 2015].
- Fanti, F. and Catuneanu, O. (2009): Stratigraphy of the Upper Cretaceous Wapiti Formation, west-central Alberta, Canada; Canadian Journal of Earth Sciences, v. 46, no. 4, p. 263–286.
- Fenton, M.M., Waters, E.J., Pawley, S.M., Atkinson, N., Utting, D.J. and McKay, K. (2013): Surficial geology of Alberta; Alberta Energy Regulator, AER/AGS Map 601, scale 1: 1 000 000, URL <[http://ags.aer.ca/publications/MAP\\_601.html](http://ags.aer.ca/publications/MAP_601.html)> [June 2015].
- Gabert, G.M. and Roed, M.A. (1968): Bedrock topography and surficial aquifers, Edson area, Alberta; Research Council of Alberta, Earth Sciences Report 1968-1, URL <[http://ags.aer.ca/publications/ESR\\_1968\\_01.html](http://ags.aer.ca/publications/ESR_1968_01.html)> [June 2015].
- Geiger, K.W. (1965): Bedrock topography of southwestern Alberta; Research Council of Alberta, Earth Sciences Report 1965-1, URL <[http://ags.aer.ca/publications/ESR\\_1965\\_01.html](http://ags.aer.ca/publications/ESR_1965_01.html)> [September 2016].
- Gibson, D.W. (1977): Upper Cretaceous and Tertiary coal-bearing strata in the Drumheller-Ardley region, Red Deer River valley, Alberta; Geological Survey of Canada, Paper 76-35, 41 p.
- Grasby, S.E., Chen, Z., Hamblin, A.P., Wozniak, P.R. and Sweet, A.R. (2008): Regional characterization of the Paskapoo bedrock aquifer system, southern Alberta; Canadian Journal of Earth Sciences, v. 45, no. 12, p. 1501–1516.
- Gravenor, C.P. and Bayrock, L.A. (1961): Glacial deposits of Alberta; Royal Society of Canada Special Publication, v. 3, p. 33–50.
- Hathway, B. (2011): Late Maastrichtian paleovalley systems in west-central Alberta: mapping the Battle Formation in the subsurface; Canadian Society of Petroleum Geologists Bulletin, v. 59, no. 3, p. 195–206.
- Howard, A.D. (1960): Cenozoic history of northeastern Montana and northwestern North Dakota with emphasis on the Pleistocene; U.S. Geological Survey, Professional Paper 326, 108 p.

- Hughes, A.T., Smerdon, B.D. and Alessi, D.S. (2017): Summary of hydraulic conductivity values for the Paskapoo Formation in west-central Alberta; Alberta Energy Regulator, AER/AGS Open File Report 2016-03, 25 p, URL <[http://ags.aer.ca/publications/OFR\\_2016\\_03.html](http://ags.aer.ca/publications/OFR_2016_03.html)> [March 2017].
- Irish, E.J.W. (1970): The Edmonton Group of south-central Alberta; *Bulletin of Canadian Petroleum Geology*, v.18, no. 2, p. 125–155.
- Jackson, L. E., Phillips, F.M., Shimamura, K. and Little, E.C. (1997): Cosmogenic  $^{36}\text{Cl}$  dating of the Foothills erratics train, Alberta, Canada; *Geology*, v. 25, p. 195–198.
- Jackson, L. E., Phillips, F.M. and Little, E.C. (1999): Cosmogenic  $^{36}\text{Cl}$  dating of the maximum limit of the Laurentide Ice Sheet in southwestern Alberta; *Canadian Journal of Earth Sciences*, v. 36, p. 1347–1356.
- Johnson, E.G. and Johnson, L.A. (2012): Hydraulic fracture water usage in northeast British Columbia: locations, volumes and trends; *in* Geoscience reports 2012, British Columbia Ministry of Energy and Mines, p. 41–63, URL <<http://www2.gov.bc.ca/gov/content/industry/natural-gas-oil/petroleum-geoscience/petroleum-geoscience-publications/geoscience-reports/geoscience-2012>> [February 2017].
- Leckie, D.A. (2006): Tertiary fluvial gravels and evolution of the western Canadian prairie landscape; *Sedimentary Geology*, v. 190, p. 139–158.
- Lelliott, M.R., Cave, M.R. and Wealthall, G.P. (2009): A structured approach to the measurement of uncertainty in 3D geological models; *Quarterly Journal of Engineering Geology and Hydrogeology*, v. 42, p. 95–105.
- Lennox, D.H. (1966): The preglacial Edson buried-valley aquifer; Alberta Research Council, Open File Report 1966-02, URL <[http://ags.aer.ca/publications/OFR\\_1966\\_02.html](http://ags.aer.ca/publications/OFR_1966_02.html)> [June 2015].
- Lerbekmo, J.F. and Sweet, A.R. (2008): Magnetostratigraphy and biostratigraphy of the continental Paleocene in the Calgary area, southwestern Alberta; *Bulletin of Canadian Petroleum Geology*, v. 48, no. 4, p. 285–306.
- Levson, V.M. and Rutter, N.W. (1996): Evidence of Cordilleran Late Wisconsinan glaciers in the ‘ice-free corridor’; *Quaternary International*, v. 32, p. 33–51.
- Liverman, D.G.E. (1989): The Quaternary geology of the Grande Prairie area Alberta; Ph.D. thesis, University of Alberta, 360 pp.
- Liverman, D.G.E., Catto, N. and Rutter, N. (1989): Laurentide glaciation in west-central Alberta: a single (Late Wisconsinan) event; *Canadian Journal of Earth Sciences*, NRC Research Press, v. 26, no. 2, p. 266–274.
- Lyster, S. and Andriashek, L.D. (2012): Geostatistical rendering of the architecture of hydrostratigraphic units within the Paskapoo Formation, central Alberta; Energy Resources Conservation Board/, ERCB/AGS Bulletin 66, 103 p, URL <[http://ags.aer.ca/publications/BUL\\_066.html](http://ags.aer.ca/publications/BUL_066.html)> [July 2016].
- MacCormack, K.E., Brodeur, J.J. and Eyles, C.H. (2013): Evaluating the impact of data quantity, distribution and algorithm selection on the accuracy of 3D subsurface models using synthetic grid models of varying complexity; *Journal of Geographical Systems*, v. 15, no. 1, p. 71–88.
- MacCormack, K.E., Atkinson, N. and Lyster, S. (2015): Bedrock topography of Alberta, Canada; Alberta Energy Regulator, AER/AGS Map 602, scale 1:1 000 000, URL <[http://ags.aer.ca/publications/MAP\\_602.html](http://ags.aer.ca/publications/MAP_602.html)> [June 2015].
- Maxey, G.B. (1964): Hydrostratigraphic Units; *Journal of Hydrology*, v. 2, p. 124–129.

- Morgan, A.J., Paulen, R.C., Slattery, S.R. and Froese, C.R. (2012): Geological setting for large landslides at the Town of Peace River, Alberta (NTS 84C); Energy Resources Conservation Board, ERCB/AGS OFR 2012-04, 33 p, URL <[http://ags.aer.ca/publications/OFR\\_2012\\_04.html](http://ags.aer.ca/publications/OFR_2012_04.html)> [February, 2017].
- Pawley, S.M. and Atkinson, N. (2013): Surficial geology of the Little Smoky area (NTS 83K/NW); Alberta Geological Survey, Map 564, scale 1:100 000, URL <[http://ags.aer.ca/publications/MAP\\_564.html](http://ags.aer.ca/publications/MAP_564.html)> [June 2015].
- Pettapiece, W.W. (1986): Physiographic subdivisions of Alberta; Land Resources Research Centre, Research Branch, Agriculture Canada, scale 1:1 500 000.
- Prior, G.J., Hathway, B., Glombick, P.M., Paná, D.I., Banks, C.J., Hay, D.C., Schneider, C.L., Grobe, M., Elgr, R. and Weiss, J.A. (2013): Bedrock geology of Alberta; Alberta Energy Regulator, AER/AGS Map 600, scale 1:1 000 000, URL <[http://ags.aer.ca/publications/MAP\\_600.html](http://ags.aer.ca/publications/MAP_600.html)> [June 2015].
- Rivard, C., Lavoie, D., Lefebvre, R., Séjourné, S., Lamontagne, C. and Duchesne, M. (2014): An overview of Canadian shale gas production and environmental concerns; International Journal of Coal Geology, v. 126, p. 64–76.
- Roed, M.A. (1968): Surficial geology of the Edson-Hinton area, Alberta; Ph.D. thesis, University of Alberta, 201 p.
- Roed, M.A. (1975): Cordilleran and Laurentide multiple glaciation west-central Alberta, Canada; Canadian Journal of Earth Sciences, NRC Research Press, v. 12, no. 9, p. 1493–1515.
- Seaber, P.R. (1988): Hydrostratigraphic units; *in* Back, W., Rosenchein, J.R. and Seaber, P.R., Hydrogeology, The Geology of North America, Geological Society of America, v. 0-2, pp. 9-14.
- Smerdon, B.D., Atkinson, L.A., Hartman, G.M.D., Playter, T.L. and Andriashek, L.D. (2016): Field evidence of nested groundwater flow along the Little Smoky River, west-central Alberta; Alberta Energy Regulator, AER/AGS Open File Report 2016-02, 34 p., URL <[http://ags.aer.ca/OFR\\_2016\\_02.html](http://ags.aer.ca/OFR_2016_02.html)> [May 2016].
- Stalker, A.M. (1956). The erratics train, foothills of Alberta; Geological Survey of Canada, Bulletin 37, 31 p.
- St-Onge, D.A. (1972): Sequence of glacial lakes in north-central Alberta; Geological Survey of Canada, Bulletin 213, 16 p.
- Utting, D.J. (2012): Surficial geology of the Meekwap Lake area (NTS 83K/NE); Energy Resources Conservation Board, ERCB/AGS Map 559, scale 1:100 000, URL <[http://ags.aer.ca/publications/MAP\\_559.html](http://ags.aer.ca/publications/MAP_559.html)> [June 2015].
- Utting, D.J. (2013): Surficial geology of the Fox Creek area (NTS83K/SE); Energy Resources Conservation Board, ERCB/AGS Map 562, scale 1:100 000, URL <[http://ags.aer.ca/publications/MAP\\_562.html](http://ags.aer.ca/publications/MAP_562.html)> [June 2015].
- Utting, D.J., Atkinson, N. and Pawley, S. (2015): Reconstruction of proglacial lakes in Alberta; Canadian Quaternary Association 2015 Conference, St. John's, Newfoundland, August 16–19, abstracts, p. 82.
- Utting, D.J., Atkinson, N., Pawley, S. and Livingstone, S.J. (2016): Reconstructing the confluence zone between Laurentide and Cordilleran ice sheets along the Rocky Mountain Foothills, southwest Alberta; Journal of Quaternary Science, v. 31, p.769–787.
- Vonhof, J.A. (1969): Tertiary gravels and sands in the Canadian Great Plains; Ph.D. thesis, University of Saskatchewan, 279 p.

- Westgate, J.A., Fritz, P., Matthews, J.V., Jr., Kalas, L. and Green, R. (1971): Sediments of mid-Wisconsinan age in west-central Alberta; geochronology, insects, ostracodes, mollusca, and the oxygen isotope composition of molluscan shells; Geological Society of America, Rocky Mountain Section Annual Meeting, abstracts with program, v. 3, p. 419.
- Westgate, J.A., Fritz, P., Matthews, J.V., Jr., Kalas, L., Delorme, L.D., Green, R. and Aario, R. (1972): Geochronology and paleoecology of mid-Wisconsinan sediments in west-central Alberta; International Geological Congress, 24<sup>th</sup> session, abstracts, p. 380.